

CANNABIS USE DISORDER AND RESTING STATE FUNCTIONAL CONNECTIVITY

**INVESTIGATING RESTING STATE FUNCTIONAL CONNECTIVITY IN
CANNABIS USE DISORDER INDIVIDUALS USING HUMAN
CONNECTOME PROJECT DATA.**

Author: Peter Najdzionek B.A.

A thesis submitted to the School of Graduate Studies in partial fulfilment of the
requirements for the Degree Master of Science

Descriptive Note

McMaster University, MASTERS OF SCIENCE (2022), Hamilton, ON.

DEPARTMENT: NEUROSCIENCE

TITLE: Investigating Resting State Functional Connectivity in Cannabis Use Disorder
Individuals Using Human Connectome Project Data.

AUTHOR: Peter Najdzionek B.A.

SUPERVISOR: James MacKillop, Ph.D.

PAGE COUNT: ix, 43

LAY ABSTRACT

Cannabis Use Disorder (CUD) is the recent Diagnostic and Statistical Manual diagnosis for problematic cannabis use. Cannabis is known to impact both cognition and the structure of the brain, but the underpinnings of CUD are unknown. One historically successful approach to investigating psychological disorders is evaluating patterns of associations at rest in three distinct brain networks: the task positive, default mode, and salience networks. These networks are integral to cognitive control and function. Using Human Connectome Project Young Adult (HCP-YA) data, these brain networks were analysed in CUD individuals and healthy controls. Differences in brain activity were found across all three networks. The three brain networks in CUD individuals exhibited a regression to random activity within the occipital lobe, an area of the brain associated with vision. Additionally, the task-positive and default mode network in CUD individuals exhibited decreased brain activity within the respective networks.

ABSTRACT

PURPOSE: The triple-network model of psychopathology theorizes psychological disorders manifest from aberrant functional connectivity in three major brain networks, the central executive network, default mode network, and salience network. To date, no research has used this framework to investigate resting-state functional connectivity in cannabis users using fMRI technology. Since attentional deficits have been associated with cannabis use, the dorsal attention network was an additional network of interest.

METHODS: Using Human Connectome Project Young Adults (HCP-YA) data, 34 CUD individuals were matched to 34 controls using propensity score matching, resulting in 68 participants with brain data (M_{age} : 27.2, 17.6% female). Functional connectivity was assessed using CONN, a MATLAB-based extension package for Statistical Parameter Mapping 12 (SPM12) dedicated to assessing and displaying functional connectivity using fMRI technology. A seed-to-voxel technique was used, with *a priori* regions of interest (ROI) derived from CONN's library of ROI. Significant clusters exceeded a voxel threshold of $p < .0001$ FDR-correction, and $p < .001$ cluster threshold.

RESULTS: CUD individuals had aberrant functional connectivity across the default mode network, salience network, and dorsal attention network. A consistent finding across networks was weaker anti-correlation with the occipital cortex. Both the default mode network and dorsal attention network exhibited weaker positive connectivity with surrounding areas and pre-/post-central gyrus. The salience network in CUD individuals uniquely exhibited greater connectivity, with greater positive connectivity between the right supramarginal gyrus and left inferior frontal gyrus / precentral gyrus / central opercular cortex, and greater anti-correlation between the left insula and right postcentral gyrus.

CONCLUSION: The triple-network approach to CUD revealed systemic differences across networks; but may not be the best model for understanding CUD biomarkers. The results highlight functional brain connectivity with problematic cannabis usage.

Acknowledgements

First I'd like to thank my supervisor Dr. James MacKillop. I have always been appreciative of your attention and passion for research during our meetings. Without your leadership and guidance, I would not be the budding scientist I am today. Working with you is a delight, and it's a primary reason why I'm continuing as a Ph.D. student at McMaster University.

Second, I'd like to thank my other committee members, Dr. Iris Balodis and Dr. Michael Van Ameringen. The process was quite challenging and at times I doubted myself and the project, but with your advisement and insight I was able to prevail.

Third, I'd like to thank my "Brain Friends", Carly, Tegan, and Emma. Moving to a new city (and a new country) during COVID was extremely difficult. Whether I need to vent frustrations to a friend, or I'm struggling with some fMRI concept, I know I can reach out to you. I'm beyond grateful for our relationship both as colleagues and friends.

Lastly, I'd like to thank and acknowledge everyone who has supported me along my journey through life. Whether you're an immediate family member, close friend, or past mentor, if you're reading this of your own volition, you had a profound impact on my life. You made me who I am, and I wouldn't be here without you.

Table of Contents

Descriptive Note	ii
Lay Abstract	iii
Abstract	iv
Acknowledgements	v
Table of Contents	vi
List of Tables	vii
List of Figures	viii
List of abbreviations and symbols	ix
Declaration of Academic Achievement	xi
Introduction	1
Methods	6
Participants	6
MRI data acquisition and processing	9
Results	11
Default Mode Network	11
Task Positive Network	11
Salience Network	12
Discussion	13
References	18
Appendix 1: Tables and Figures	26

List of Tables

Table 1a – Sample demographics	26
Table 1b – Sample demographics	27
Table 2 – Default mode network significant clusters	28
Table 3 – Task positive network significant clusters	39
Table 4 – Salience network significant clusters	30

List of Figures

Figure 1a – Distribution of propensity scores	31
Figure 1b – Differences in propensity scores	32
Figure 2-3 – Visualization of significant clusters from DMN	33
Figure 4-6 – Visualization of significant clusters from dorsal attention network	35
Figure 7-8 – Visualization of significant clusters from salience network	38
Figure 9-12 – Visualization of ROIs	40

List of abbreviations and symbols

ACC	Anterior Cingulate Cortex
ANCOVA	Analysis of Covariance
ANOVA	Analysis of Variance
BMI	Body Mass Index
BOLD	Blood Oxygen Level Dependent
CBD	Cannabidiol
CB ₁	Cannabinoid receptor
CONN	CONN Functional Connectivity Toolbox
CUD	Cannabis Use Disorder
DLPFC	Dorsolateral Prefrontal Cortex
DMN	Default Mode Network
DSM	Diagnostic and Statistical Manual
EEG	Electroencephalogram
fALFF	fractional Amplitude of Low-Frequency Fluctuations
FDR	False Discovery Rate
fMRI	functional Magnetic Resonance Imaging
FWHM	Full Width at Half Maximum
HC	Healthy Control
HCP	Human Connectome Project
HCP-YA	Human Connectome Project Young Adults
MATLAB	Matrix Laboratory
MNI	Montreal Neurological Institute
mPFC	Medial Prefrontal Cortex
MRI	Magnetic Resonance Imaging
PCC	Posterior Cingulate Cortex
ROI	Region of Interest
T ₁	Longitudinal Relaxation Time

THC

Tetrahydrocannabinol

Declaration of Academic Achievement

All data was extracted from Human Connectome Project Young Adults, with permission from the HCP consortium. Functional connectivity analyses were performed in CONN, using an altered publicly available macro-processing script (*conn_batch_humanconnectome.m*). Research and analyses design were a collaboration between Peter Najdzionek and Dr. James MacKillop. All analyses, figures, and manuscripts were conducted / created by Peter Najdzionek.

Introduction

Cannabis users and consumption continues to rise in North America. Within the United States, 9% of US adults 18 years or older used cannabis within the past year (Hasin et al., 2015; United Nations, 2022), while 25% of Canadians age 16 or older reported using cannabis within the past year (Health Canada, 2021). Young adults (age 18-25) are the largest demographic to report cannabis use (Substance Abuse and Mental Health Services Administration, 2020; Callaghan et al., 2019). As more individuals use cannabis, some will begin to use cannabis problematically. Health Canada (2018) estimated 33% of cannabis users will experience problems due to their cannabis usage, with frequently cited epidemiological reports concurring (United Nations, 2022; Hasin et al., 2015; Conner et al., 2021). One way to quantify ‘problematic substance usage’, is using DSM-V Substance Use Disorder diagnoses. Cannabis Use Disorder (CUD) requires two out of ten criteria (persisting for at least one year), primarily focused on cannabis-related behaviors (e.g. attempts to quit, using more than intended, withdrawal, increased tolerance), and continued consumption despite social and physiological problems (American Psychiatric Association, 2013).

The neurobiological underpinnings of CUD are not fully understood. Cannabis contains phytocannabinoids (e.g. delta-9-tetrahydrocannabinol (THC) and cannabidiol (CBD)) which act on cannabinoid 1 and 2 receptors (CB1r, CB2r); a majority of CB1r are found in the brain, while a majority of CB2r are found in the immune system (Di Marzo & Piscitelli, 2015; Ferland & Hurd, 2020). Acute intoxication of cannabis (more specifically THC) is known to impair verbal learning and memory, attention, psychomotor function, and inhibition (Broyd et al., 2016). These diminished cognitive abilities along with physiological research, such as positron emission

topographical evidence of CB1r downregulation associated with cannabis usage (Hirvonen et al., 2012), indicate cannabis fundamentally alters the brain. However, there is no clear neurobiological indicator between CUD individuals and non-problematic cannabis users.

One way to assess brain activity and brain differences between two populations, is measuring functional connectivity within the brain. Neurons that fire synchronously are thought to be communicating, regardless of proximity. Coupled neurons are grouped into networks associated with their function; thus neurons are functionally connected. An early example mapped functional connectivity between the two separate areas of the brain (now known as the primary and supplemental motor areas) during a finger taping task (Biswal et al., 1995). Ultimately, research has revealed several different and unique networks (Uddin et al., 2019; Witt et al., 2021), with resting state fMRI (measuring brain activity at rest) becoming a popular method of measuring functional connectivity.

Resting state functional connectivity of cannabis users has previously been investigated with varying results. A recent systematic review of fMRI resting-state functional connectivity in cannabis users found 40% of studies reported greater positive functional connectivity in cannabis users between frontal regions, fronto-temporal, and fronto-striatal regions (Thomson et al., 2022). While informative, the review did not find consistent results. For example, four studies included in the review investigated functional connectivity with the orbitofrontal cortex, as previous studies found cannabis users have reduced orbitofrontal cortical thickness (Wittemann et al., 2021; Harper et al., 2021); all studies included in the systematic review found unique different results. One study found cannabis users had *increased* positive connectivity with the temporal lobe (Filbey et al., 2014), another study found cannabis users had *decreased* positive connectivity with the parietal lobe (Lopez-Larson et al., 2015), while a third study found no

differences in functional connectivity associated with cannabis usage (Subramaniam et al., 2018). The systematic review was limited in nature due to numerous heterogeneous methodologies (Thomson et al., 2022); different resting state analysis techniques (seed-to-voxel, independent component analysis, graph theory, fractional amplitude of low frequency fluctuations, etc.) and varying cannabis metrics (definitions of cannabis user, required abstinence, etc.) made direct comparison impossible. Increased stringency is necessary to summarizing cannabis-related resting state functional connectivity literature.

DSM-V CUD diagnosis is a simple way to clarify ‘cannabis user’. While this approach polarizes and dichotomizes cannabis users into problematic and unproblematic users, it alleviates arbitrary definitions of cannabis users based on cannabis consumption over time (e.g. cannabis users must use cannabis >10 times a month). Furthermore, understanding functional brain connectivity between CUD and non-CUD individuals may reveal a biomarker for CUD, which may further our understanding of the neurobiological basis of CUD.

Relatively few studies have contrasted brain functional connectivity of individuals with cannabis-related diagnoses to non-cannabis users. Eight studies exclusively defined their cannabis group by DSM-IV (or DSM-5) diagnosis, without co-occurring psychological disorders such as bipolar disorder or schizophrenia; six of the studies used seed-to-voxel resting state methods, while one study used fractional amplitude of low-frequency fluctuations (fALFF) (Orr et al., 2013), and one used graph theory (Koenis et al., 2020). The seed-to-voxel approach identifies a region of interest (ROI) and correlates its fluctuating BOLD signal with every voxel; the correlated voxels are grouped into clusters of similar brain activity as the ROI. However, these correlations do not convey information of the BOLD signal; the fALFF approach converts the BOLD signal into a power spectrum, to analyze the physical properties of the brain activity

(Zou et al., 2008). Finally, the graph theory approach uses information theory to analyze various aspects of defined brain networks (Bullmore & Sporns, 2009).

For the sake of homogeneity and direct comparability, only the six seed-to-voxel fMRI studies were assessed. Five of studies compared individuals with cannabis dependence or abuse diagnoses to non-using or cannabis naïve individuals. Most studies investigated the reward network, a brain network comprising primarily of limbic brain areas, with supplementing frontal brain regions (Höflich et al., 2018). A 2017 longitudinal study found cannabis dependent adolescents had deteriorating functional connectivity between the caudal ACC and DLPFC (Camchong et al., 2017). Later, the same lab conducted a longitudinal study on young adult cannabis users and found problematic cannabis users experienced lower functional connectivity between the caudal ACC and medial dorsal thalamus, superior frontal gyrus, and middle frontal gyrus; the dorsal ACC exhibited similar decreased functional connectivity with the medial frontal gyrus and superior frontal gyrus (Camchong et al., 2019). In 2018, a study found group differences in brain connectivity between the striatum (dorsal and ventral seeds) and the rostral anterior cingulate cortex, in addition to the dorsal medial prefrontal cortex (Zhou et al., 2018). The three studies insinuate CUD is associated with a dysfunctional reward network, however one study found no significant differences in subcortical functional connectivity between cannabis dependent individuals and controls (Manza et al., 2018). While the thalamus is not integral to the reward network, a 2019 study segmented thalamic nuclei and found group differences in functional connectivity differences between the nuclei and their projected destination (Demiral et al., 2019). Only the most recent study used DSM-5 criteria (instead of DSM-IV cannabis dependence or abuse) and found CUD individuals experienced aberrant functional connectivity from the amygdala, PCC, and ACC (Aloi et al., 2021). Together, these six studies demonstrate

disruption of functional brain connectivity among cannabis dependent individuals, particularly in the frontal and striatal regions.

Prior research investigated cannabis use disorder through the lens of dysfunctional reward pathways, while neglecting an established theoretical approach: the triple network theory. The triple network theory identifies three major brain networks responsible for psychiatric disorders: the central executive network, the default mode network, and the salience network. In theory, psychiatric disorders are associated with abnormal functional connectivity within or between one (or more) of the networks (Menon, 2011; Menon, 2019). The central executive network is responsible for executive functions and consists of the middle frontal gyrus, anterior inferior parietal lobe, and intraparietal sulcus (Menon, 2011; Uddin et al., 2019). The default mode network is activated during rest or tasks requiring self-reflection, and consists of the medial prefrontal cortex, posterior cingulate cortex, and lateral inferior parietal lobe (Menon, 2011; Uddin et al., 2019). The salience network is responsible for detecting salient stimuli and activating other brain networks; major nodes in the salience network include the anterior insula and ACC (Menon, 2011; Uddin et al., 2019). This framework has elucidated depressive, schizophrenic, bipolar, neurodevelopmental, and neurocognitive disorders (Wang et al., 2020; Li et al.; 2021; Hull et al., 2017; Nicholson et al., 2020a; Gürsel et al., 2018, Bos et al., 2017; Liang et al., 2021; Li et al., 2019). Expanded to substance use disorders, one previous study found a relationship between distress tolerance (a co-occurring behavior with substance use disorder), cocaine usage, and brain functional connectivity (Reese et al., 2019). Furthermore, a recent EEG study used the triple network framework, and found increased functional connectivity in problematic cannabis users between nodes of the salience and central executive network

(Imperator et al., 2020). However, to date, no study has used the triple network framework to investigate fMRI functional connectivity associated with cannabis use disorder.

The current study sought to bridge this gap in scientific knowledge by using publicly available data and resources to investigate functional connectivity associated with cannabis use disorder. Brain and behavioral data were acquired from the Human Connectome Project Young Adult dataset (HCP-YA), an open science consortium focused on developing human connectomes (Van Essen et al., 2013). The HCP-YA dataset is large, with more than 1100 participants, 800 measures, and extensive resting-state fMRI data; additionally, HCP is well established with over 1500 publications using HCP data (Elam et al., 2021). Using the triple-network framework theory of psychopathology, CUD individuals were expected to differ in functional connectivity in the three different networks (central executive network, DMN, and salience network). Since cannabis usage is associated with attentional deficits (Scott et al., 2018), the dorsal attention network was also investigated; the dorsal attention network and central executive network were analyzed together as a ‘task-positive network’. While no specific hypotheses of cortical areas with aberrant functional connectivity were created, based on previous research, CUD individuals were expected to have altered connectivity in the frontal cortex, and altered functional connectivity between nodes of the central executive network and salience network (Camchong et al., 2017; Camchong et al., 2019; Imperatori et al., 2020; Zhou et al., 2018).

Methods

Participants

Participants' data were extracted from the Human Connectome Project Young Adults dataset (HCP-YA). HCP-YA participants were between the ages of 22 to 35, relatively healthy (no documented history of psychiatric disorder, substance abuse, neurological, or cardiovascular disease), and cognitively able (able to give informed consent and passed the Mini Mental Status Exam); notable exclusion criteria included participants' history of seizures, significant brain trauma, or premature birth. Exact inclusion / exclusion criteria for HCP-YA is detailed in the original publication (Van Essen et al., 2012). Participants were not given abstinence instructions prior to participation.

Five measures of cannabis are captured by HCP-YA: 1) If the participant ever used cannabis; 2) Participant's age of first use (stratified into four age groups, spanning adolescence and early adulthood); 3) Cumulative lifetime cannabis usage (bucketed into 6 quantities: 0, 1-5, 6-10, 11-100, 101-1000, 1001+ times); 4) Prior history of DSM-IV cannabis dependence diagnosis, derived from the Semi-Structured Assessment for the Genetics of Alcoholism – II (SSAGA-II)(Bucholz et al., 1994); 5) THC metabolites found in urinary drug screen administered prior to MRI scan. Problematic cannabis-users were defined as individuals who tested positive for THC and met criteria for cannabis dependence during their lifetime. The dual-criteria definition of CUD is advantageous, as THC positivity does not indicate cannabis dependence, and lifetime history of dependence does not indicate current cannabis usage; concurring THC positivity and history of cannabis dependence indicates current problematic cannabis usage. Of the HCP-YA population, 43 participants were THC+ with a history of cannabis dependence; 3 participants were excluded for missing brain imaging files or incomplete data, an additional 6 participants were excluded due to inaccessible data via server outages. The final sample consisted of 34 problematic cannabis users.

Problematic cannabis users were matched to participants with previous cannabis exposure, who never met criteria for cannabis dependence and were THC- prior to the MRI scan. Matching was executed via propensity scores using the ‘MatchIt’ R package (version 4.2.0). Every participant was assigned a propensity score, which measured the probability of the participant’s diagnosis based on defined covariates (i.e. age, gender, socioeconomic status, education, and BMI) (Austin, 2011). Using the nearest-neighbor method, CUD participants were matched to non-CUD participants with the closest propensity score. Matching successfully decreased the mean propensity score differences on all matching criteria except BMI (see Figure 1b), t-tests concluded the final sample did not statistically differ between their matched criteria ($p > .05$). The resulting group demographics can be found in Tables 1a & 1b. T-tests conducted on non-matched variables indicated age of first cannabis use, but not anxiety and depression scores, differed between groups ($p < .05$).

After all brain analyses were completed, the sample was further analyzed for other substance use. Current and past substance use was assessed via SSAGA-II, past substance use differed between groups, see Table 1b. Both t-tests and Wilcoxon rank sum tests suggested nicotine dependence (Fagerström Test for Nicotine Dependence scores) or DSM-IV alcohol dependence did not differ between groups ($p > .05$). However CUD-individuals were more likely to use alcohol problematically; CUD individuals had higher rates of past or present DSM-IV alcohol abuse diagnosis (Wilcoxon: $W = 391$, $p = 0.002$; T-test: $t = -3.2719$, $p = 0.002$), and had more symptoms of alcohol abuse (Wilcoxon: $W = 316.5$, $p < 0.001$; T-test: $t = -4.109$, $p < 0.001$) and dependence (Wilcoxon: $W = 401$, $p = 0.012$; T-test: $t = -2.2939$, $p = 0.025$). Breathalyzer results confirmed no participants were impaired by alcohol (blood alcohol content $< .05$). Five of the 68 participants tested positive for illicit substances beyond cannabis; one non-CUD

individual tested positive for opiates, one CUD participant was positive for both opiates & methamphetamines, one CUD participant was positive for amphetamines, and 2 CUD individuals tested positive for oxycontin.

MRI data acquisition and processing

HCP extensively pre-processed resting-state data was used for analyses. The pre-processed data is produced from the standard HCP structural and functional pipelines (Glasser et al., 2013), in addition to the HCP resting-state pipeline (Smith et al., 2013). Explained briefly, the HCP structural pipeline produced T1 images, corrected bias field, and normalized T1 images to MNI space; the HCP functional pipeline removed spatial distortions, realigned functional images offset by motion, co-registered structural and functional images, minimized bias field signal, and normalized the timeseries to a global mean; the HCP resting-state pipeline focused on temporal corrections: removed scanner drift via highpass filtering, and identified and regressed out artifact from the data. Exact parameters (e.g. structural and functional echo-planar imaging sequencing parameters, alignment approach, determination of field bias, etc.) are found in the original manuscripts (Glasser et al., 2013; Smith et al., 2013). HCP resting state data collected brain activity isolated to one hemisphere in 15-minute intervals. Ultimately, one hour of resting state data (an aggregated 5,000 timepoints collected) was collected and preprocessed. Due to the computational requirements and volume of data, only 30 minutes of resting state data was used in analyses.

fMRI analyses were conducted in CONN, a MATLAB based program designed for investigating functional brain connectivity. The CONN *conn_batch_humanconnectome.m* script,

a publicly available macro-processing script created specifically for HCP-YA extensively pre-processed resting state data, was altered and executed. The script was adapted to the current study in the following ways: 1) decreased the amount of data processed to 30 minutes of resting state; 2) restricted functional connectivity analyses to *a priori* ROIs, using whole brain seed-to-voxel analysis; 3) changed functional smoothing kernel to 3mm FWHM. CONN's predetermined ROIs were used to investigate three different functional networks: default mode network (seeds in: medial prefrontal cortex, lateral parietal lobe, and posterior cingulate cortex), salience network (seeds in: anterior cingulate cortex, insula, rostral prefrontal cortex, and supramarginal gyrus), and task positive network with the dorsal attention and central executive subnetworks (dorsal attention seeds: bilateral frontal eye fields and intra-parietal sulcus; central executive seeds: bilateral lateral prefrontal cortex and posterior parietal cortex). Visualization for the seeds are found in Figures 9-12.

The script pipeline was segmented into three distinct steps: preprocessing, denoising, and analyses. Preprocessing consisted of segmentation of the brain (white matter, grey matter, cerebral spinal fluid, etc.), identification of movement over .9mm between frames (or BOLD signal change greater than five standard deviations), and application of a functional smoothing kernel of 3mm. Denoising constructed weighted general linear models using CONN's default weighting (hrf-weighting), regressed nuisance covariates (white matter, cerebral spinal fluid, realignment, and scrubbing), applied a bandpass filter [.01, .1], and detrended data via linear regression. First-level analyses correlated the timeseries between the regions of interest (ROI) and every voxel, and transformed all connectivity values using Fisher's r-Z transformation. Second-level analyses identified clusters differing from zero across all participants, with significant voxels and clusters surviving $p < .0001$ FDR-corrected voxel threshold, and $p < .001$

FDR-corrected cluster threshold while being at least 10 voxels. Results were parceled using the Automated Anatomical Labeling Atlas (Tzourio-Mazoyer et al., 2002). Group differences were calculated in RStudio; since the groups were matched, one-way ANOVAs were conducted (as opposed to ANCOVAs for common covariates such as education and income).

Results

Default Mode Network

Of the four default mode network seeds, two seeds had functional connectivity differences between CUD individuals and controls, see Table 2 and Figures 2&3. CUD individuals exhibited weaker dysconnectivity (negativity correlated brain connectivity) between the posterior cingulate cortex and the right inferior frontal gyrus (pars opercularis), and left precentral gyrus. CUD individuals also displayed weaker dysconnectivity between the right lateral parietal and the right occipital pole, and left precentral gyrus. Weaker positive connectivity was exhibited by CUD individuals between the right lateral parietal and a large area of the precuneus. This large cluster underwent post hoc analyses to determine the strongest signal of the cluster. The voxel threshold was increased until the cluster was under 500 voxels. At a voxel threshold of 1×10^{-8} , the cluster covered 438 voxels of the precuneus; an ANOVA determined CUD individuals retained decreased positive functional connectivity, $F(1,66) = 4.02$, $p = .045$. No group differences in functional connectivity were found from the medial prefrontal cortex and left lateral parietal.

Task Positive Network

Functional connectivity of the task positive network was altered in CUD individuals, particularly the dorsal attention network. Three of the four nodes of the dorsal attention network

had significantly difference functionally connectivity between CUD individuals and controls, see Table 3 and Figures 4-6; there were no group differences in functional connectivity for the central executive network. CUD individuals had weaker dysconnectivity between bilateral intra-parietal sulcus and occipital cortex; the left intra-parietal sulcus had weak connectivity with both the left and right occipital pole, while the right intra-parietal sulcus had dysconnectivity unique to the right occipital pole. Additionally, CUD individuals exhibited decreased positive connectivity. The left frontal eye-fields lacked connectivity with a large cluster (2381 voxels) spanning the left central gyrus (pre- and post-) / supramarginal gyrus, the right superior parietal lobe, and left central opercular cortex. The left intra-parietal sulcus had weaker functional connectivity with a large cluster (4172 voxels) spanning the left superior parietal lobe / post central gyrus / supramarginal gyrus / occipital cortex, and the right cerebellum⁸. Both large clusters were reduced to 500 voxels by increasing the voxel threshold, but functional connectivity did not differ between groups ($p > .05$). Finally, the right intra-parietal sulcus had weaker positive connectivity with the left central opercular cortex. No differences in functional connectivity were found from the right frontal eye fields, bilateral lateral prefrontal cortex, or bilateral posterior parietal cortex.

Saliency Network

The salience network also had functional connectivity differences between groups, see Table 4 and Figures 7&8. The left insula had weaker negative connectivity with the left occipital cortex, and stronger negative connectivity with the right postcentral gyrus ($F(1,66) = 5.63$, $p = .021$). CUD individuals exhibited greater positive connectivity between the right supramarginal gyrus and brain strip covering the left inferior frontal gyrus (pars opercularis) / precentral gyrus /

and central opercular cortex. No differences in functional connectivity were exhibited by the ACC, right insula, bilateral rostral prefrontal cortex, or bilateral supramarginal gyrus.

Discussion

This is the first study to examine fMRI resting state functional connectivity in CUD individuals using the triple network framework of psychopathology. Supporting our hypotheses, functional connectivity differences were exhibited in CUD individuals across all multiple brain networks. A majority of the differences occurred in the task positive network, specifically the dorsal attention network, where CUD individuals had weaker functional connectivity with the occipital lobe, regions of the temporal lobe, pre- and post-central gyrus, cerebellum, and areas immediately outside the seed regions. The DMN also demonstrated weaker functional connectivity from the right lateral parietal lobe and posterior cingulate cortex, with the occipital lobe, pre- and post-central gyrus, and inferior frontal gyrus. The salience network hosted the fewest connectivity differences between groups, while uniquely exhibiting greater functional connectivity among the CUD group.

Across all networks, CUD individuals exhibited weaker negative connectivity with areas of the occipital lobe. Among the task positive network and default mode network this dysconnectivity was isolated to regions in the parietal lobe (bilateral intra-parietal sulci and right lateral parietal lobe, respectively), the salience network exhibited dysconnectivity between the left insula and occipital lobe. While unexpected, previous studies found similar findings, with problematic cannabis users displaying patterns of dysconnectivity with the occipital lobe (Pujol et al., 2014; Aloï et al., 2021). However, one previous study investigated CUD functional connectivity of the thalamus and found no significant differences between the occipital lobe and their preceding thalamic nuclei (Demiral et al., 2019). Additional research is required for

understanding impact of this anti-correlation, and if behavioral consequences are associated with the deficits.

The pre-/post-central gyrus is another area of differing connectivity across multiple networks. CUD individuals exhibited weaker positive functional connectivity from the task positive network and DMN, while the salience network had stronger connectivity in both directions (negative and positive association). These findings add to previous literature indicating aberrant pre-/post-central gyrus functional connectivity associated with cannabis usage (Camchong et al., 2019; Aloï et al., 2021). Multiple resting state studies with participants receiving THC dosing reported THC-related decreases in functional connectivity with the central gyrus (Demiral et al., 2019; Wall et al., 2019). It is clear CUD individuals experience broad functional disrupted connectivity with pre-/post-central gyrus.

The final finding shared across multiple networks, is altered connectivity with lateral areas in the frontal lobe. Within the task positive network, the dorsal-attention network had decreased positive functional connectivity with the central opercular cortex. The pars opercularis of the inferior frontal gyrus exhibited weaker negative connectivity to the DMN's posterior cingulate cortex, and stronger positive connectivity with the salience network's right supramarginal gyrus. This result is supported by at least 2 studies which found similar weak anti-correlation between the PCC and inferior frontal gyrus associated with cannabis usage (Wall et al., 2019; Pujol et al., 2014). However, the decreased functional connectivity between the dorsal-attention network and central opercular cortex is novel, with no prior research reporting this finding.

In sum, framing CUD with the triple-network model yielded varying results. Of the three major networks (DMN, CEN, and salience network) implicated in the theoretical model, CUD

exhibited aberrant functional connectivity from nodes in the DMN and salience network; no differences were found in CEN nodes. However, most brain connectivity differences were experienced in the dorsal attention network, a brain network neglected by the triple network model; additionally, most connectivity differences were experienced beyond network nodes (i.e. with the central gyrus and occipital cortex), instead of between network nodes. Given these results, CUD cannot adequately be defined by aberrant connectivity between or within three specific networks, as the triple network model suggests. Instead, CUD has similar patterns of weaker functional connectivity with the central gyrus, occipital lobe, and lateral frontal lobe across a multitude of networks. This notion is supported by a recent CUD study which found similar patterns of altered connectivity with the central gyrus and occipital cortex, from brain areas responsible for emotion processing (Aloi et al., 2021).

These results begin to clarify neurobiological biomarkers for CUD, and how CUD differs from casual cannabis usage. Previous research related to cannabis usage found both functional and structural differences in frontal and striatal brain regions (Owens et al., 2022; Thomson et al., 2022; Wittemann et al., 2021; Newman et al., 2020). Studies comparing CUD individuals to non-cannabis-using individuals reported similar findings (Camchong et al., 2019; Camchong et al., 2017; Zhou et al., 2018). These previous CUD findings neglected casual cannabis users, thus the results may reflect a drug effect of cannabis, rather than functional connectivity unique to CUD individuals. The current study identified functional connectivity indicative of problematic cannabis usage, by contrasting CUD individuals to individuals who have previously used cannabis. The results of the current study suggest problematic cannabis behavior and CUD may be identifiable by a lack of global functional connectivity with the occipital cortex and central gyrus.

The results of the current study must be considered with its the strengths and weaknesses. One strength is the quality of the data. The current study used 30 minutes of resting state data, significantly longer than standard resting state studies. The large amount of data combined with the adequate sample size of 68, greatly increased the statistical power of the results. Additionally, the voxel and cluster thresholds for group level analyses (.0001 FDR corrected and .001 FDR corrected, respectfully) were extremely conservative, more stringent than the literature standard (.001 uncorrected, and .05 FDR corrected). The quantity of significant clusters despite the restrictive approach demonstrates robust and strong differences in brain connectivity for CUD individuals. Furthermore the sample was statistically matched, ensuring observed effects are not attributable to covariates such as education, income or BMI. Lastly, while not an inherent strength of the study, the use of open-source resources ensures the results are replicable.

While this study has strengths, it still has limitations. A large limitation is the study's definition of CUD individual. The definition of CUD individuals arose from two criteria, a lifetime history of cannabis dependence and THC+ urinary screening. A lifetime history of cannabis dependence is not a current diagnosis of cannabis dependence; thus, it's possible some CUD individuals included in the sample were previously problematic cannabis users, but now engage with cannabis in a non-problematic manner. Furthermore cannabis dependence is the antecedent of CUD, while the criteria overlap significantly, the diagnoses are separate and our results may not accurately reflect CUD. Future studies should be vigilant about substance use metrics; the current study was limited by outdated substance metrics, which cannot address novel concerns such as concurrent substance usage, cannabis administration, or cannabis potency. Finally, this study is cross-sectional and cannot determine the directionality of the relationship between aberrant functional connectivity and problematic cannabis behavior.

In conclusion, this study used HCP-YA data to investigate functional connectivity associated with CUD. Patterns of aberrant functional connectivity existed, with CUD individuals having decreased in functional connectivity exhibited by the dorsal-attention network and DMN, and increased functional connectivity from the salience network. Evidence of altered anticorrelation with the occipital lobe and pre-/post-central gyrus existed across all networks. These results provide an initial framework for analyzing CUD through the lens of the triple-network theory of psychopathology. Further understanding CUD and its neuro-psychological basis may lead to biofeedback therapies aimed at correcting aberrant functional connectivity (Nicholson et al., 2020b).

References

- Aloi, J., McCusker, M. C., Lew, B. J., Schantell, M., Eastman, J. A., Frenzel, M. R., & Wilson, T. W. (2021). Altered amygdala-cortical connectivity in individuals with Cannabis use disorder. *Journal of Psychopharmacology*, *35*(11), 1365–1374.
<https://doi.org/10.1177/02698811211054163>
- American Psychiatric Association. (2013). *Diagnostic and statistical manual of mental disorders* (5th ed.). <https://doi.org/10.1176/appi.books.9780890425596>
- Austin, P. C. (2011). An Introduction to Propensity Score Methods for Reducing the Effects of Confounding in Observational Studies. *Multivariate Behavioral Research*, *46*(3), 399–424. <https://doi.org/10.1080/00273171.2011.568786>
- Batalla, A., Bos, J., Postma, A., & Bossong, M. G. (2021). The Impact of Cannabidiol on Human Brain Function: A Systematic Review. *Frontiers in Pharmacology*, *11*, 618184.
<https://doi.org/10.3389/fphar.2020.618184>
- Bélangier, M., Allaman, I., & Magistretti, P. J. (2011). Brain Energy Metabolism: Focus on Astrocyte-Neuron Metabolic Cooperation. *Cell Metabolism*, *14*(6), 724–738.
<https://doi.org/10.1016/j.cmet.2011.08.016>
- Biswal, B., Zerrin Yetkin, F., Haughton, V. M., & Hyde, J. S. (1995). Functional connectivity in the motor cortex of resting human brain using echo-planar mri. *Magnetic Resonance in Medicine*, *34*(4), 537–541. <https://doi.org/10.1002/mrm.1910340409>
- Blanco-Hinojo, L., Pujol, J., Harrison, B. J., Macià, D., Batalla, A., Nogué, S., Torrens, M., Farré, M., Deus, J., & Martín-Santos, R. (2017). Attenuated frontal and sensory inputs to the basal ganglia in cannabis users. *Addiction Biology*, *22*(4), 1036–1047.
<https://doi.org/10.1111/adb.12370>
- Bos, D. J., Oranje, B., Achterberg, M., Vlaskamp, C., Ambrosino, S., de Reus, M. A., van den Heuvel, M. P., Rombouts, S. A. R. B., & Durston, S. (2017). Structural and functional connectivity in children and adolescents with and without attention deficit/hyperactivity disorder. *Journal of Child Psychology and Psychiatry*, *58*(7), 810–818.
<https://doi.org/10.1111/jcpp.12712>
- Bossier, H., Roels, S. P., Seurinck, R., Banaschewski, T., Barker, G. J., Bokde, A. L. W., Quinlan, E. B., Desrivières, S., Flor, H., Grigis, A., Garavan, H., Gowland, P., Heinz, A., Ittermann, B., Martinot, J.-L., Artiges, E., Nees, F., Orfanos, D. P., Poustka, L., ... Moerkerke, B. (2020). The empirical replicability of task-based fMRI as a function of sample size. *NeuroImage*, *212*, 116601.
<https://doi.org/10.1016/j.neuroimage.2020.116601>
- Bossong, M. G., van Hell, H. H., Schubart, C. D., van Saane, W., Iseger, T. A., Jager, G., van Osch, M. J. P., Jansma, J. M., Kahn, R. S., Boks, M. P., & Ramsey, N. F. (2019). Acute

- effects of Δ^9 -tetrahydrocannabinol (THC) on resting state brain function and their modulation by COMT genotype. *European Neuropsychopharmacology*, 29(6), 766–776. <https://doi.org/10.1016/j.euroneuro.2019.03.010>
- Broyd, S. J., van Hell, H. H., Beale, C., Yücel, M., & Solowij, N. (2016). Acute and Chronic Effects of Cannabinoids on Human Cognition—A Systematic Review. *Biological Psychiatry*, 79(7), 557–567. <https://doi.org/10.1016/j.biopsych.2015.12.002>
- Bucholz, K. K., Cadoret, R., Cloninger, C. R., Dinwiddie, S. H., Hesselbrock, V. M., Nurnberger, J. I., Jr, Reich, T., Schmidt, I., & Schuckit, M. A. (1994). A new, semi-structured psychiatric interview for use in genetic linkage studies: a report on the reliability of the SSAGA. *Journal of studies on alcohol*, 55(2), 149–158. <https://doi.org/10.15288/jsa.1994.55.149>
- Bullmore, E., & Sporns, O. (2009). Complex brain networks: Graph theoretical analysis of structural and functional systems. *Nature Reviews Neuroscience*, 10(3), 186–198. <https://doi.org/10.1038/nrn2575>
- Callaghan, R. C., Sanches, M., Benny, C., Stockwell, T., Sherk, A., & Kish, S. J. (2019). Who consumes most of the cannabis in Canada? Profiles of cannabis consumption by quantity. *Drug and Alcohol Dependence*, 205, 107587. <https://doi.org/10.1016/j.drugalcdep.2019.107587>
- Camchong, J., Collins, P. F., Becker, M. P., Lim, K. O., & Luciana, M. (2019). Longitudinal Alterations in Prefrontal Resting Brain Connectivity in Non-Treatment-Seeking Young Adults With Cannabis Use Disorder. *Frontiers in Psychiatry*, 10, 514. <https://doi.org/10.3389/fpsy.2019.00514>
- Camchong, J., Lim, K. O., & Kumra, S. (2016). Adverse Effects of Cannabis on Adolescent Brain Development: A Longitudinal Study. *Cerebral Cortex*, bhw015. <https://doi.org/10.1093/cercor/bhw015>
- Camchong, J., Lim, K. O., & Kumra, S. (2017). Adverse Effects of Cannabis on Adolescent Brain Development: A Longitudinal Study. *Cerebral Cortex (New York, NY)*, 27(3), 1922–1930. <https://doi.org/10.1093/cercor/bhw015>
- Connor, J. P., Stjepanović, D., Le Foll, B., Hoch, E., Budney, A. J., & Hall, W. D. (2021). Cannabis use and cannabis use Disorder. *Nature Reviews. Disease Primers*, 7(1), 16. <https://doi.org/10.1038/s41572-021-00247-4>
- Crane, N. A., & Phan, K. L. (2021). Effect of Δ^9 -Tetrahydrocannabinol on frontostriatal resting state functional connectivity and subjective euphoric response in healthy young adults. *Drug and Alcohol Dependence*, 221, 108565. <https://doi.org/10.1016/j.drugalcdep.2021.108565>
- Demiral, Ş. B., Tomasi, D., Wiers, C. E., Manza, P., Shokri-Kojori, E., Studentsova, Y., Wang, G.-J., & Volkow, N. D. (2019). Methylphenidate's effects on thalamic metabolism and functional connectivity in cannabis abusers and healthy controls.

- Neuropsychopharmacology*, 44(8), 1389–1397. <https://doi.org/10.1038/s41386-018-0287-2>
- Di Marzo, V., & Piscitelli, F. (2015). The Endocannabinoid System and its Modulation by Phytocannabinoids. *Neurotherapeutics*, 12(4), 692–698. <https://doi.org/10.1007/s13311-015-0374-6>
- Elam, J. S., Glasser, M. F., Harms, M. P., Sotiropoulos, S. N., Andersson, J. L. R., Burgess, G. C., Curtiss, S. W., Oostenveld, R., Larson-Prior, L. J., Schoffelen, J.-M., Hodge, M. R., Cler, E. A., Marcus, D. M., Barch, D. M., Yacoub, E., Smith, S. M., Ugurbil, K., & Van Essen, D. C. (2021). The Human Connectome Project: A retrospective. *NeuroImage*, 244, 118543. <https://doi.org/10.1016/j.neuroimage.2021.118543>
- Ferland, J.-M. N., & Hurd, Y. L. (2020). Deconstructing the neurobiology of cannabis use disorder. *Nature Neuroscience*, 23(5), 600–610. <https://doi.org/10.1038/s41593-020-0611-0>
- Filbey, F. M., Aslan, S., Calhoun, V. D., Spence, J. S., Damaraju, E., Caprihan, A., & Segall, J. (2014). Long-term effects of marijuana use on the brain. *Proceedings of the National Academy of Sciences*, 111(47), 16913–16918. <https://doi.org/10.1073/pnas.1415297111>
- Fox, M. D., & Raichle, M. E. (2007). Spontaneous fluctuations in brain activity observed with functional magnetic resonance imaging. *Nature Reviews Neuroscience*, 8(9), 700–711. <https://doi.org/10.1038/nrn2201>
- Glasser, M. F., Sotiropoulos, S. N., Wilson, J. A., Coalson, T. S., Fischl, B., Andersson, J. L., Xu, J., Jbabdi, S., Webster, M., Polimeni, J. R., Van Essen, D. C., & Jenkinson, M. (2013). The minimal preprocessing pipelines for the Human Connectome Project. *NeuroImage*, 80, 105–124. <https://doi.org/10.1016/j.neuroimage.2013.04.127>
- Grimm, O., Löffler, M., Kamping, S., Hartmann, A., Rohleder, C., Leweke, M., & Flor, H. (2018). Probing the endocannabinoid system in healthy volunteers: Cannabidiol alters fronto-striatal resting-state connectivity. *European Neuropsychopharmacology*, 28(7), 841–849. <https://doi.org/10.1016/j.euroneuro.2018.04.004>
- Gürsel, D. A., Avram, M., Sorg, C., Brandl, F., & Koch, K. (2018). Frontoparietal areas link impairments of large-scale intrinsic brain networks with aberrant fronto-striatal interactions in OCD: A meta-analysis of resting-state functional connectivity. *Neuroscience & Biobehavioral Reviews*, 87, 151–160. <https://doi.org/10.1016/j.neubiorev.2018.01.016>
- Harper, J., Wilson, S., Malone, S. M., Hunt, R. H., Thomas, K. M., & Iacono, W. G. (2021). Orbitofrontal cortex thickness and substance use disorders in emerging adulthood: Causal inferences from a co-twin control/discordant twin study. *Addiction (Abingdon, England)*, 116(9), 2548–2558. <https://doi.org/10.1111/add.15447>
- Harris, J. C., Wallace, A. L., Thomas, A. M., Wirtz, H. G., Kaiver, C. M., & Lisdahl, K. M. (2022). Disrupted Resting State Attentional Network Connectivity in Adolescent and

- Young Adult Cannabis Users following Two-Weeks of Monitored Abstinence. *Brain Sciences*, 12(2), 287. <https://doi.org/10.3390/brainsci12020287>
- Hasin, D. S., Saha, T. D., Kerridge, B. T., Goldstein, R. B., Chou, S. P., Zhang, H., Jung, J., Pickering, R. P., Ruan, W. J., Smith, S. M., Huang, B., & Grant, B. F. (2015). Prevalence of Marijuana Use Disorders in the United States Between 2001-2002 and 2012-2013. *JAMA Psychiatry*, 72(12), 1235–1242. <https://doi.org/10.1001/jamapsychiatry.2015.1858>
- Health Canada. (2018, March 2). *Addiction to cannabis* [Education and awareness]. <https://www.canada.ca/en/health-canada/services/drugs-medication/cannabis/health-effects/addiction.html>
- Health Canada. (2021, December 23). *Canadian Cannabis Survey 2021: Summary* [Surveys]. <https://www.canada.ca/en/health-canada/services/drugs-medication/cannabis/research-data/canadian-cannabis-survey-2021-summary.html>
- Hirjak, D., Schmitgen, M. M., Werler, F., Wittmann, M., Kubera, K. M., Wolf, N. D., Sambataro, F., Calhoun, V. D., Reith, W., & Wolf, R. C. (2022). Multimodal MRI data fusion reveals distinct structural, functional and neurochemical correlates of heavy cannabis use. *Addiction Biology*, 27(2), e13113. <https://doi.org/10.1111/adb.13113>
- Hirvonen, J., Goodwin, R., Li, C.-T., Terry, G., Zoghbi, S., Morse, C., Pike, V., Volkow, N., Huestis, M., & Innis, R. (2012). Reversible and regionally selective downregulation of brain cannabinoid CB1 receptors in chronic daily cannabis smokers. *Molecular Psychiatry*, 17(6), 642–649. <https://doi.org/10.1038/mp.2011.82>
- Höflich, A., Michenthaler, P., Kasper, S., & Lanzenberger, R. (2018). Circuit Mechanisms of Reward, Anhedonia, and Depression. *International Journal of Neuropsychopharmacology*, 22(2), 105–118. <https://doi.org/10.1093/ijnp/pyy081>
- Hull, J. V., Dokovna, L. B., Jacokes, Z. J., Torgerson, C. M., Irimia, A., & Van Horn, J. D. (2017). Resting-State Functional Connectivity in Autism Spectrum Disorders: A Review. *Frontiers in Psychiatry*, 7, 205. <https://doi.org/10.3389/fpsy.2016.00205>
- Imperatori, C., Massullo, C., Carbone, G. A., Panno, A., Giacchini, M., Capriotti, C., Lucarini, E., Ramella Zampa, B., Murillo-Rodríguez, E., Machado, S., & Farina, B. (2020). Increased Resting State Triple Network Functional Connectivity in Undergraduate Problematic Cannabis Users: A Preliminary EEG Coherence Study. *Brain Sciences*, 10(3), 136. <https://doi.org/10.3390/brainsci10030136>
- Klumpers, L. E., Cole, D. M., Khalili-Mahani, N., Soeter, R. P., te Beek, E. T., Rombouts, S. A. R. B., & van Gerven, J. M. A. (2012). Manipulating brain connectivity with δ 9-tetrahydrocannabinol: A pharmacological resting state fMRI study. *NeuroImage*, 63(3), 1701–1711. <https://doi.org/10.1016/j.neuroimage.2012.07.051>
- Koenis, M. M. G., Durnez, J., Rodrigue, A. L., Mathias, S. R., Alexander-Bloch, A. F., Barrett, J. A., Doucet, G. E., Frangou, S., Knowles, E. E. M., Mollon, J., Denbow, D., Aberizk, K., Zatory, M., Janssen, R. J., Curran, J. E., Blangero, J., Poldrack, R. A., Pearlson, G. D., &

- Glahn, D. C. (2020). Associations of cannabis use disorder with cognition, brain structure, and brain function in African Americans. *Human Brain Mapping*, 42(6), 1727–1741. <https://doi.org/10.1002/hbm.25324>
- Li, C., Li, Y., Zheng, L., Zhu, X., Shao, B., Fan, G., Liu, T., Wang, J., & Initiative, and A. D. N. (2019). Abnormal Brain Network Connectivity in a Triple-Network Model of Alzheimer’s Disease. *Journal of Alzheimer’s Disease*, 69(1), 237–252. <https://doi.org/10.3233/JAD-181097>
- Li, Y., Dai, X., Wu, H., & Wang, L. (2021). Establishment of Effective Biomarkers for Depression Diagnosis With Fusion of Multiple Resting-State Connectivity Measures. *Frontiers in Neuroscience*, 15, 729958. <https://doi.org/10.3389/fnins.2021.729958>
- Liang, S., Wang, Q., Greenshaw, A. J., Li, X., Deng, W., Ren, H., Zhang, C., Yu, H., Wei, W., Zhang, Y., Li, M., Zhao, L., Du, X., Meng, Y., Ma, X., Yan, C.-G., & Li, T. (2021). Aberrant triple-network connectivity patterns discriminate biotypes of first-episode medication-naïve schizophrenia in two large independent cohorts. *Neuropsychopharmacology*, 46(8), 1502–1509. <https://doi.org/10.1038/s41386-020-00926-y>
- Lopez-Larson, M. P., Rogowska, J., & Yurgelun-Todd, D. (2015). Aberrant orbitofrontal connectivity in marijuana smoking adolescents. *Developmental Cognitive Neuroscience*, 16, 54–62. <https://doi.org/10.1016/j.dcn.2015.08.002>
- Ma, L., Hettema, J. M., Cousijn, J., Bjork, J. M., Steinberg, J. L., Keyser-Marcus, L., Woisard, K., Lu, Q., Roberson-Nay, R., Abbate, A., & Moeller, F. G. (2021). Resting-State Directional Connectivity and Anxiety and Depression Symptoms in Adult Cannabis Users. *Biological Psychiatry: Cognitive Neuroscience and Neuroimaging*, 6(5), 545–555. <https://doi.org/10.1016/j.bpsc.2020.09.015>
- Manza, P., Tomasi, D., & Volkow, N. D. (2018). Subcortical local functional hyperconnectivity in cannabis dependence. *Biological Psychiatry. Cognitive Neuroscience and Neuroimaging*, 3(3), 285–293. <https://doi.org/10.1016/j.bpsc.2017.11.004>
- Martín-Santos, R., Fagundo, A. B., Crippa, J. A., Atakan, Z., Bhattacharyya, S., Allen, P., Fusar-Poli, P., Borgwardt, S., Seal, M., Busatto, G. F., & McGuire, P. (2010). Neuroimaging in cannabis use: A systematic review of the literature. *Psychological Medicine*, 40(3), 383–398. <https://doi.org/10.1017/S0033291709990729>
- Mason, N. L., Theunissen, E. L., Hutten, N. R. P. W., Tse, D. H. Y., Toennes, S. W., Stiers, P., & Ramaekers, J. G. (2019). Cannabis induced increase in striatal glutamate associated with loss of functional corticostriatal connectivity. *European Neuropsychopharmacology*, 29(2), 247–256. <https://doi.org/10.1016/j.euroneuro.2018.12.003>
- Menon, B. (2019). Towards a new model of understanding – The triple network, psychopathology and the structure of the mind. *Medical Hypotheses*, 133, 109385. <https://doi.org/10.1016/j.mehy.2019.109385>

- Menon, V. (2011). Large-scale brain networks and psychopathology: A unifying triple network model. *Trends in Cognitive Sciences*, 15(10), 483–506.
<https://doi.org/10.1016/j.tics.2011.08.003>
- Minhas, M., Murphy, C. M., Balodis, I. M., Samokhvalov, A. V., & MacKillop, J. (2021). Food addiction in a large community sample of Canadian adults: Prevalence and relationship with obesity, body composition, quality of life and impulsivity. *Addiction*, 116(10), 2870–2879. <https://doi.org/10.1111/add.15446>
- Newman, S. D., Cheng, H., Kim, D.-J., Schnakenberg-Martin, A., Dydak, U., Dharmadhikari, S., Hetrick, W., & O'Donnell, B. (2020). An investigation of the relationship between glutamate and resting state connectivity in chronic cannabis users. *Brain Imaging and Behavior*, 14(5), 2062–2071. <https://doi.org/10.1007/s11682-019-00165-w>
- Nicholson, A. A., Harricharan, S., Densmore, M., Neufeld, R. W. J., Ros, T., McKinnon, M. C., Frewen, P. A., Théberge, J., Jetly, R., Pedlar, D., & Lanius, R. A. (2020). Classifying heterogeneous presentations of PTSD via the default mode, central executive, and salience networks with machine learning. *NeuroImage : Clinical*, 27, 102262.
<https://doi.org/10.1016/j.nicl.2020.102262>
- Nicholson, A. A., Ros, T., Densmore, M., Frewen, P. A., Neufeld, R. W. J., Théberge, J., Jetly, R., & Lanius, R. A. (2020). A randomized, controlled trial of alpha-rhythm EEG neurofeedback in posttraumatic stress disorder: A preliminary investigation showing evidence of decreased PTSD symptoms and restored default mode and salience network connectivity using fMRI. *NeuroImage : Clinical*, 28, 102490.
<https://doi.org/10.1016/j.nicl.2020.102490>
- Orr, C., Morioka, R., Behan, B., Datwani, S., Doucet, M., Ivanovic, J., Kelly, C., Weierstall, K., Watts, R., Smyth, B., & Garavan, H. (2013). Altered resting-state connectivity in adolescent cannabis users. *The American Journal of Drug and Alcohol Abuse*, 39(6), 372–381. <https://doi.org/10.3109/00952990.2013.848213>
- Owens, M. M., Hyatt, C. S., Gray, J. C., Carter, N. T., MacKillop, J., Miller, J. D., & Sweet, L. H. (2019). Cortical morphometry of the five-factor model of personality: Findings from the Human Connectome Project full sample. *Social Cognitive and Affective Neuroscience*, 14(4), 381–395. <https://doi.org/10.1093/scan/nsz017>
- Pujol, J., Blanco-Hinojo, L., Batalla, A., López-Solà, M., Harrison, B. J., Soriano-Mas, C., Crippa, J. A., Fagundo, A. B., Deus, J., de la Torre, R., Nogué, S., Farré, M., Torrens, M., & Martín-Santos, R. (2014). Functional connectivity alterations in brain networks relevant to self-awareness in chronic cannabis users. *Journal of Psychiatric Research*, 51, 68–78. <https://doi.org/10.1016/j.jpsychires.2013.12.008>
- Reese, E. D., Yi, J. Y., McKay, K. G., Stein, E. A., Ross, T. J., & Daughters, S. B. (2019). Triple Network Resting State Connectivity Predicts Distress Tolerance and Is Associated with Cocaine Use. *Journal of Clinical Medicine*, 8(12), 2135.
<https://doi.org/10.3390/jcm8122135>

- Ritchay, M. M., Huggins, A. A., Wallace, A. L., Larson, C. L., & Lisdahl, K. M. (2021). Resting state functional connectivity in the default mode network: Relationships between cannabis use, gender, and cognition in adolescents and young adults. *NeuroImage: Clinical*, 30, 102664. <https://doi.org/10.1016/j.nicl.2021.102664>
- Roalf, D. R., & Gur, R. C. (2017). Functional Brain Imaging in Neuropsychology over the past 25 years. *Neuropsychology*, 31(8), 954–971. <https://doi.org/10.1037/neu0000426>
- Schnakenberg Martin, A. M., Kim, D.-J., Newman, S. D., Cheng, H., Hetrick, W. P., Mackie, K., & O'Donnell, B. F. (2021). Altered cerebellar-cortical resting-state functional connectivity in cannabis users. *Journal of Psychopharmacology*, 35(7), 823–832. <https://doi.org/10.1177/02698811211019291>
- Scott, J. C., Slomiak, S. T., Jones, J. D., Rosen, A., Moore, T. M., & Gur, R. C. (2018). Association of Cannabis With Cognitive Functioning in Adolescents and Young Adults: A Systematic Review and Meta-analysis. *JAMA psychiatry*, 75(6), 585–595. <https://doi.org/10.1001/jamapsychiatry.2018.0335>
- Seeley, W. W., Menon, V., Schatzberg, A. F., Keller, J., Glover, G. H., Kenna, H., Reiss, A. L., & Greicius, M. D. (2007). Dissociable Intrinsic Connectivity Networks for Salience Processing and Executive Control. *The Journal of Neuroscience*, 27(9), 2349–2356. <https://doi.org/10.1523/JNEUROSCI.5587-06.2007>
- Smith, S. M., Beckmann, C. F., Andersson, J., Auerbach, E. J., Bijsterbosch, J., Douaud, G., Duff, E., Feinberg, D. A., Griffanti, L., Harms, M. P., Kelly, M., Laumann, T., Miller, K. L., Moeller, S., Petersen, S., Power, J., Salimi-Khorshidi, G., Snyder, A. Z., Vu, A. T., ... Glasser, M. F. (2013). Resting-state fMRI in the Human Connectome Project. *NeuroImage*, 80, 144–168. <https://doi.org/10.1016/j.neuroimage.2013.05.039>
- Subramaniam, P., Rogowska, J., DiMuzio, J., Lopez-Larson, M., McGlade, E., & Yurgelun-Todd, D. (2018). Orbitofrontal connectivity is associated with depression and anxiety in marijuana-using adolescents. *Journal of Affective Disorders*, 239, 234–241. <https://doi.org/10.1016/j.jad.2018.07.002>
- Substance Abuse and Mental Health Services Administration. (2020). *Key Substance Use and Mental Health Indicators in the United States: Results from the 2020 National Survey on Drug Use and Health*. 156.
- Sweigert, J., Pagulayan, K., Greco, G., Blake, M., Larimer, M., & Kleinhans, N. M. (2020). A multimodal investigation of cerebellar integrity associated with high-risk cannabis use. *Addiction Biology*, 25(6), e12839. <https://doi.org/10.1111/adb.12839>
- Thomson, H., Labuschagne, I., Greenwood, L.-M., Robinson, E., Sehl, H., Suo, C., & Lorenzetti, V. (2022). Is resting-state functional connectivity altered in regular cannabis users? A systematic review of the literature. *Psychopharmacology*, 239(5), 1191–1209. <https://doi.org/10.1007/s00213-021-05938-0>

- Tzourio-Mazoyer, N., Landeau, B., Papathanassiou, D., Crivello, F., Etard, O., Delcroix, N., Mazoyer, B., & Joliot, M. (2002). Automated anatomical labeling of activations in SPM using a macroscopic anatomical parcellation of the MNI MRI single-subject brain. *NeuroImage*, *15*(1), 273–289. <https://doi.org/10.1006/nimg.2001.0978>
- Uddin, L. Q., Yeo, B. T. T., & Spreng, R. N. (2019). Towards a Universal Taxonomy of Macro-scale Functional Human Brain Networks. *Brain Topography*, *32*(6), 926–942. <https://doi.org/10.1007/s10548-019-00744-6>
- United Nations. (2022). *World Drug Report 2021*. UNITED NATIONS.
- Van Essen, D. C., Smith, S. M., Barch, D. M., Behrens, T. E. J., Yacoub, E., & Ugurbil, K. (2013). The WU-Minn Human Connectome Project: An Overview. *NeuroImage*, *80*, 62–79. <https://doi.org/10.1016/j.neuroimage.2013.05.041>
- Van Essen, D. C., Ugurbil, K., Auerbach, E., Barch, D., Behrens, T. E. J., Bucholz, R., Chang, A., Chen, L., Corbetta, M., Curtiss, S. W., Della Penna, S., Feinberg, D., Glasser, M. F., Harel, N., Heath, A. C., Larson-Prior, L., Marcus, D., Michalareas, G., Moeller, S., ... Yacoub, E. (2012). The Human Connectome Project: A data acquisition perspective. *NeuroImage*, *62*(4), 2222–2231. <https://doi.org/10.1016/j.neuroimage.2012.02.018>
- Wall, M. B., Pope, R., Freeman, T. P., Kowalczyk, O. S., Demetriou, L., Mokrysz, C., Hindocha, C., Lawn, W., Bloomfield, M. A., Freeman, A. M., Feilding, A., Nutt, D., & Curran, H. V. (2019). Dissociable effects of cannabis with and without cannabidiol on the human brain's resting-state functional connectivity. *Journal of Psychopharmacology*, *33*(7), 822–830. <https://doi.org/10.1177/0269881119841568>
- Wang, J., Wang, Y., Wu, X., Huang, H., Jia, Y., Zhong, S., Wu, X., Zhao, L., He, Y., Huang, L., & Huang, R. (2020). Shared and specific functional connectivity alterations in unmedicated bipolar and major depressive disorders based on the triple-network model. *Brain Imaging and Behavior*, *14*(1), 186–199. <https://doi.org/10.1007/s11682-018-9978-x>
- Weng, Y., Qi, R., Zhang, L., Luo, Y., Ke, J., Xu, Q., Zhong, Y., Li, J., Chen, F., Cao, Z., & Lu, G. (2019). Disturbed effective connectivity patterns in an intrinsic triple network model are associated with posttraumatic stress disorder. *Neurological Sciences*, *40*(2), 339–349. <https://doi.org/10.1007/s10072-018-3638-1>
- Wetherill, R. R., Fang, Z., Jagannathan, K., Childress, A. R., Rao, H., & Franklin, T. R. (2015). Cannabis, cigarettes, and their co-occurring use: Disentangling differences in default mode network functional connectivity. *Drug and Alcohol Dependence*, *153*, 116–123. <https://doi.org/10.1016/j.drugalcdep.2015.05.046>
- Whitfield-Gabrieli, S., Fischer, A. S., Henricks, A. M., Khokhar, J. Y., Roth, R. M., Brunette, M. F., & Green, A. I. (2018). Understanding marijuana's effects on functional connectivity of the default mode network in patients with schizophrenia and co-occurring cannabis use

- disorder: A Pilot Investigation. *Schizophrenia Research*, 194, 70–77. <https://doi.org/10.1016/j.schres.2017.07.029>
- Whitfield-Gabrieli, S., & Nieto-Castanon, A. (2012). Conn: A Functional Connectivity Toolbox for Correlated and Anticorrelated Brain Networks. *Brain Connectivity*, 2(3), 125–141. <https://doi.org/10.1089/brain.2012.0073>
- Witt, S. T., van Ettinger-Veenstra, H., Salo, T., Riedel, M. C., & Laird, A. R. (2021). What Executive Function Network is that? An Image-Based Meta-Analysis of Network Labels. *Brain Topography*, 34(5), 598–607. <https://doi.org/10.1007/s10548-021-00847-z>
- Wittemann, M., Brielmaier, J., Rubly, M., Kennel, J., Werler, F., Schmitgen, M. M., Kubera, K. M., Hirjak, D., Wolf, N. D., Reith, W., & Wolf, R. C. (2021). Cognition and Cortical Thickness in Heavy Cannabis Users. *European Addiction Research*, 27(2), 115–122. <https://doi.org/10.1159/000509987>
- Zhou, F., Zimmermann, K., Xin, F., Scheele, D., Dau, W., Banger, M., Weber, B., Hurlemann, R., Kendrick, K. M., & Becker, B. (2018). Shifted balance of dorsal versus ventral striatal communication with frontal reward and regulatory regions in cannabis-dependent males. *Human Brain Mapping*, 39(12), 5062–5073. <https://doi.org/10.1002/hbm.24345>
- Zimmermann, K., Yao, S., Heinz, M., Zhou, F., Dau, W., Banger, M., Weber, B., Hurlemann, R., & Becker, B. (2018). Altered orbitofrontal activity and dorsal striatal connectivity during emotion processing in dependent marijuana users after 28 days of abstinence. *Psychopharmacology*, 235(3), 849–859. <https://doi.org/10.1007/s00213-017-4803-6>
- Zou, Q.-H., Zhu, C.-Z., Yang, Y., Zuo, X.-N., Long, X.-Y., Cao, Q.-J., Wang, Y.-F., & Zang, Y.-F. (2008). An improved approach to detection of amplitude of low-frequency fluctuation (ALFF) for resting-state fMRI: Fractional ALFF. *Journal of Neuroscience Methods*, 172(1), 137–141. <https://doi.org/10.1016/j.jneumeth.2008.04.012>

Appendix 1: Tables and Figures

Table 1a. Participant demographic characteristics – Matched covariates

	CUD individuals	HC	Total Sample	<i>T value</i>	<i>P value</i>
Age in Years (M [SD])	27.3 [3.4]	27.2 [3.3]	27.2 [3.3]	-.11	.91
Sex Ratio (M/F)	27/7	29/5	56/12	-	-
Race (% White)	58.8%	73.5%	66.2%	-	-
Education level in Years (M [SD])	14.1 [1.88]	14.2 [2.04]	14.2 [1.95]	.25	.81
Annual Household Income Bracket (M [SD])	4.2 [2.26]	4.3 [2.15]	4.2 [2.19]	.27	.78
<\$20,000 (% of group)	32.3%	17.6%	25.0%		
\$20,000-\$39,999	29.4%	47.0%	38.2%		
\$40,000-\$74,999	17.6%	14.7%	16.1%		
>\$75,000	20.7%	20.7%	20.7%		
BMI (M [SD])	26.1 [4.05]	26.9 [4.24]	26.5 [4.14]	.83	.41

Note. M = mean. SD = standard deviation. CUD = cannabis use disorder. HC = healthy control. Reported percentages for Annual Household Income Bracket were condensed from 8 brackets to 4 brackets for brevity.

Table 1b. Participant demographic characteristics – Non-matched covariates

	CUD individuals	Ctrl	Total Sample	T value	P value
Anxiety (M [SD])	4.5 [3.54]	4.0 [2.62]	4.3 [3.10]	-.70	.49
Depression (M [SD])	5.9 [5.15]	4.1 [2.84]	5.0 [4.22]	-1.75	.09
Age range of first cannabis use (M [SD])*	1.85 [0.82]	2.88 [0.84]	2.37 [0.98]	5.09	<.001
<14 years (% of group)	38.2%	3.0%	20.6%		
15-17 years	41.2%	32.4%	36.7%		
18-20 years	17.6%	38.2%	27.9%		
21+ years	3.0%	26.4%	14.8%		
Lifetime cannabis usage (M [SD])*	4.59 [.66]	1.79 [1.04]	3.19 [1.65]	-13.3	<.001
1-5 times (% of group)	-	58.8%	29.4%		
6-10 times	-	8.8%	4.4%		
11-100 times	8.8%	26.5%	17.6%		
101-1000 times	23.5%	5.9%	14.7%		
1000+ times	67.7%	-	33.9%		
Past cocaine usage (M [SD])*	1.29 [2.11]	.06 [.24]	.68 [1.62]	-3.39	.002
Past hallucinogen usage (M [SD])*	1.56 [1.94]	.09 [.29]	.82 [1.56]	-4.37	<.001
Past opiate usage (M [SD])*	1.59 [2.12]	.03 [.17]	.81 [1.69]	-4.27	<.001
Past sedative usage (M [SD])*	1.50 [2.16]	.03 [.17]	.76 [1.69]	-3.95	<.001
Past stimulant usage (M [SD])*	1.15 [1.86]	.12 [.33]	.63 [1.42]	-3.17	.003

Note. M = mean. SD = standard deviation. CUD = cannabis use disorder. HC = healthy control. Past substance use was bucketed in the following way: 0 times = 0; 1-5 times = 1; 5+ times = 5

*Variable is statistically different between groups (2-tailed T-test, $p < .05$)

Table 2. Table of significant clusters from Default Mode Network.

Original Seed	Group difference	Direction of association	Cluster Location	# of Voxels	MNI Space (X,Y,Z)	F value	P value
LP(r)	CUD < HC	Negative	Right Occipital Pole	170	(28, -88, 18)	4.016784	0.049156
		Negative	Left Precentral Gyrus	11	(-50, -12, 52)	7.350791	0.008536
		Positive	Precuneus / Cingulate Gyrus	2832	(16, -56, 20)	5.098369	0.027261
PCC	CUD < HC	Negative	Right Inferior Frontal Gyrus / Right pars Opercularis	90	(48, 06, 22)	5.079922	0.027531
		Negative	Left Precentral Gyrus	22	(-48, -12, 54)	4.214916	0.044038

Note. LP = Lateral Parietal. PCC = Posterior Cingulate Cortex.

Table 3. Table of significant clusters from Task Positive Network.

Original Seed	Group difference	Direction of association	Cluster Location	# of Voxels	MNI Space (X,Y,Z)	F value	P value
FEF(l)	CUD < HC	Positive	Left Pre-/Post-central Gyrus, Superior Parietal Lobe	2381	(-28, -08, 60)	5.117049	0.026991
		Positive	Right Superior Parietal Lobe	196	(42, -46, 58)	4.061087	0.047958
		Positive	Left Central Opercular Cortex	23	(-38, -04, 16)	5.552336	0.021434
IPS(l)	CUD < HC	Positive	Left Superior Parietal Lobe, Postcentral Gyrus, Supramarginal Gyrus, Lateral Occipital Cortex	4172	(-62, -24, 42)	4.182232	0.044841
		Positive	Right Cerebellum8	59	(18, -74, -52)	4.845279	0.031224
		Negative	Left Occipital Pole	128	(-06, -96, 26)	5.499285	0.022041
		Negative	Right Occipital Pole	13	(16, -90, 30)	7.613396	0.00749
		Positive	Left Central Opercular Cortex	32	(-40, -04, 14)	4.668537	0.034355
IPS(r)	CUD < HC	Negative	Right Occipital Pole	20	(12, -96, 20)	5.485842	0.022197

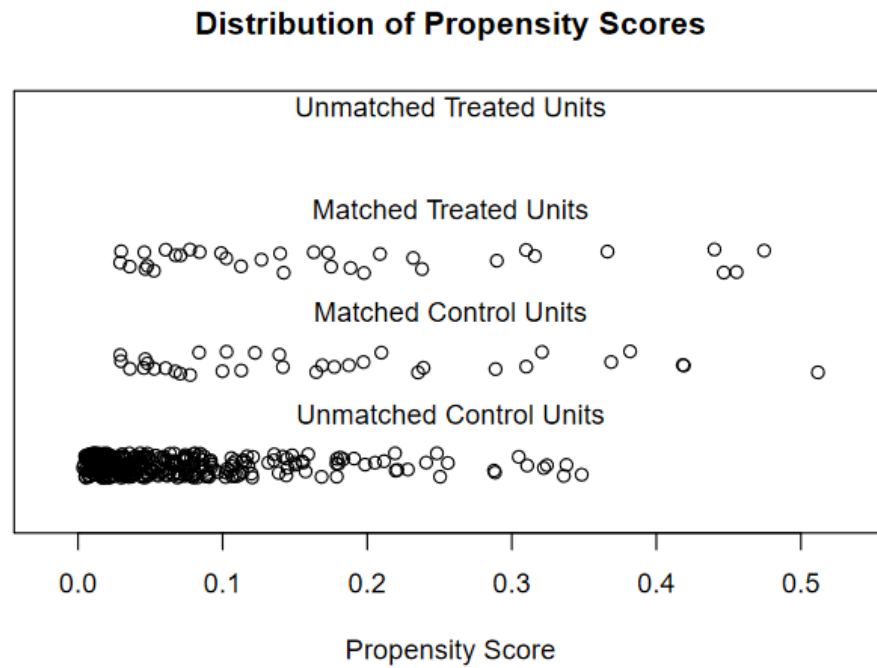
Note. FEF = Frontal Eye Fields. IPS = Intra-Partial Sulcus.

Table 4. Table of significant clusters from Salience Network.

Original Seed	Group difference	Direction of association	Cluster Location	# of Voxels	MNI Space (X,Y,Z)	F value	P value
Insula(I)	CUD < HC	Negative	Left Lateral Occipital Cortex	66	(-40, -74, 46)	5.935442	0.017546
	CUD > HC	Negative	Right Postcentral Gyrus	25	(44, -34, 62)	5.630662	0.02057
SMG(I)	CUD > HC	Negative	Left Pars Opercularis, Precentral gyrus, central opercular cortex	173	(-58, 06, -02)	7.588555	0.007583

Note. SMG = Supra-Marginal Gyrus.

Figure 1a. Distribution of propensity scores after matching



Note. CUD individuals are “treated units”

Figure 1b. Difference in propensity score for matched covariates

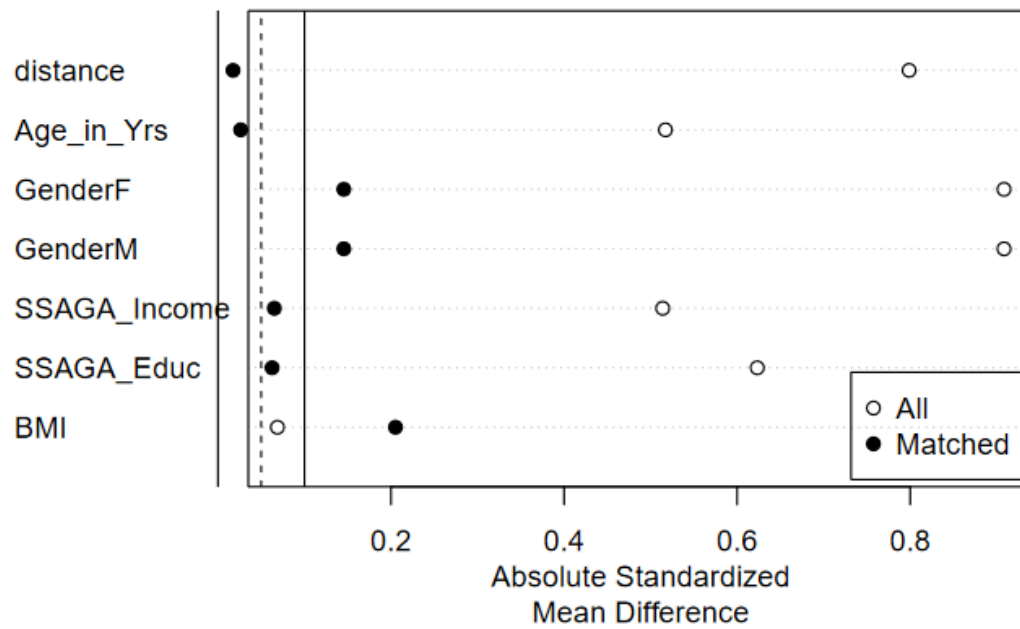
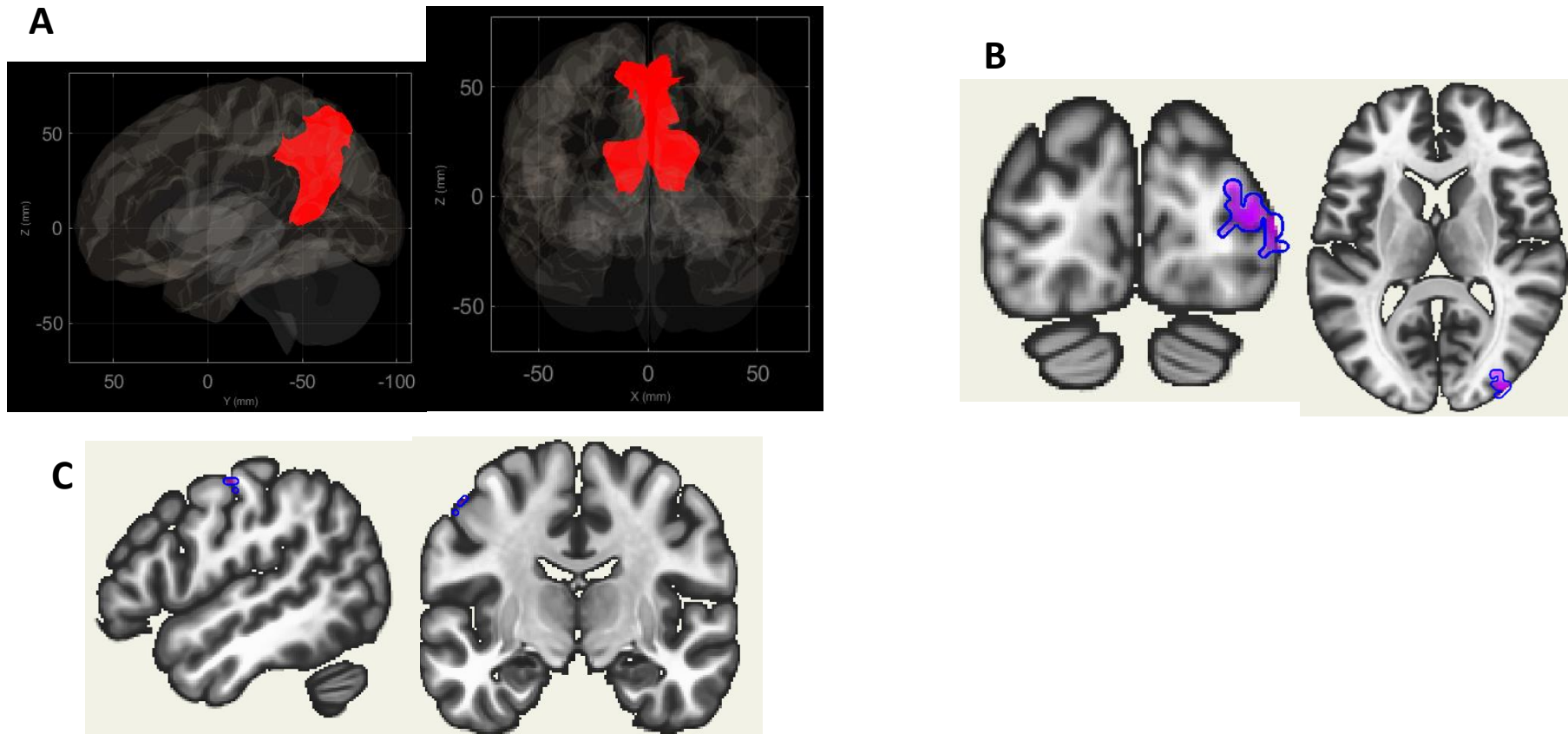
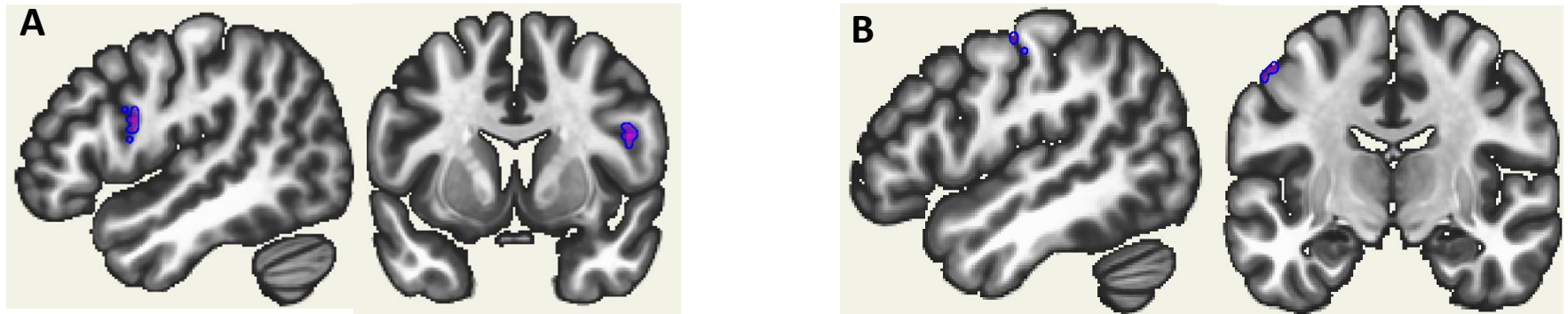


Figure 2. Visualization of significant clusters from DMN – right lateral parietal lobe



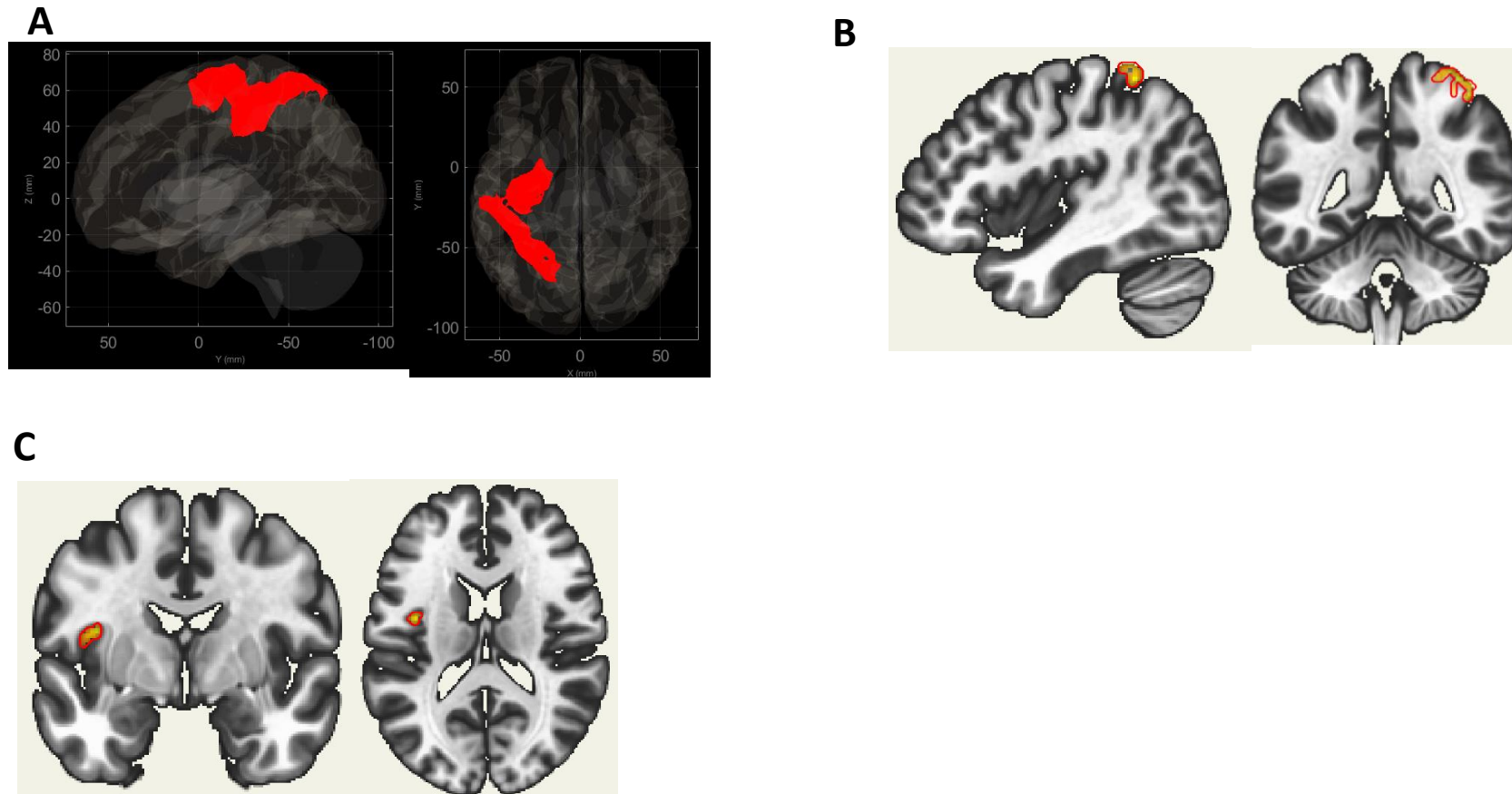
Note. The orientation (axial, sagittal, or coronal) corresponds to the best visualization of clusters. In some cases, visualizations were displayed in a 3D rendered glass brain (distinguished by a black background); two slices would not be a sufficient visualization of the entire cluster. **A)** 2832 voxel cluster with peak correlation from (16, -56, 20), located in the precuneus and parts of the PCC. **B)** 170 voxel cluster with peak correlation from (28, -88, 18), located in the right occipital pole. **C)** 11 voxel cluster with peak correlation from (-50, -12, 52), located in the left precentral gyrus.

Figure 3. Visualization of significant clusters from DMN – Posterior cingulate cortex



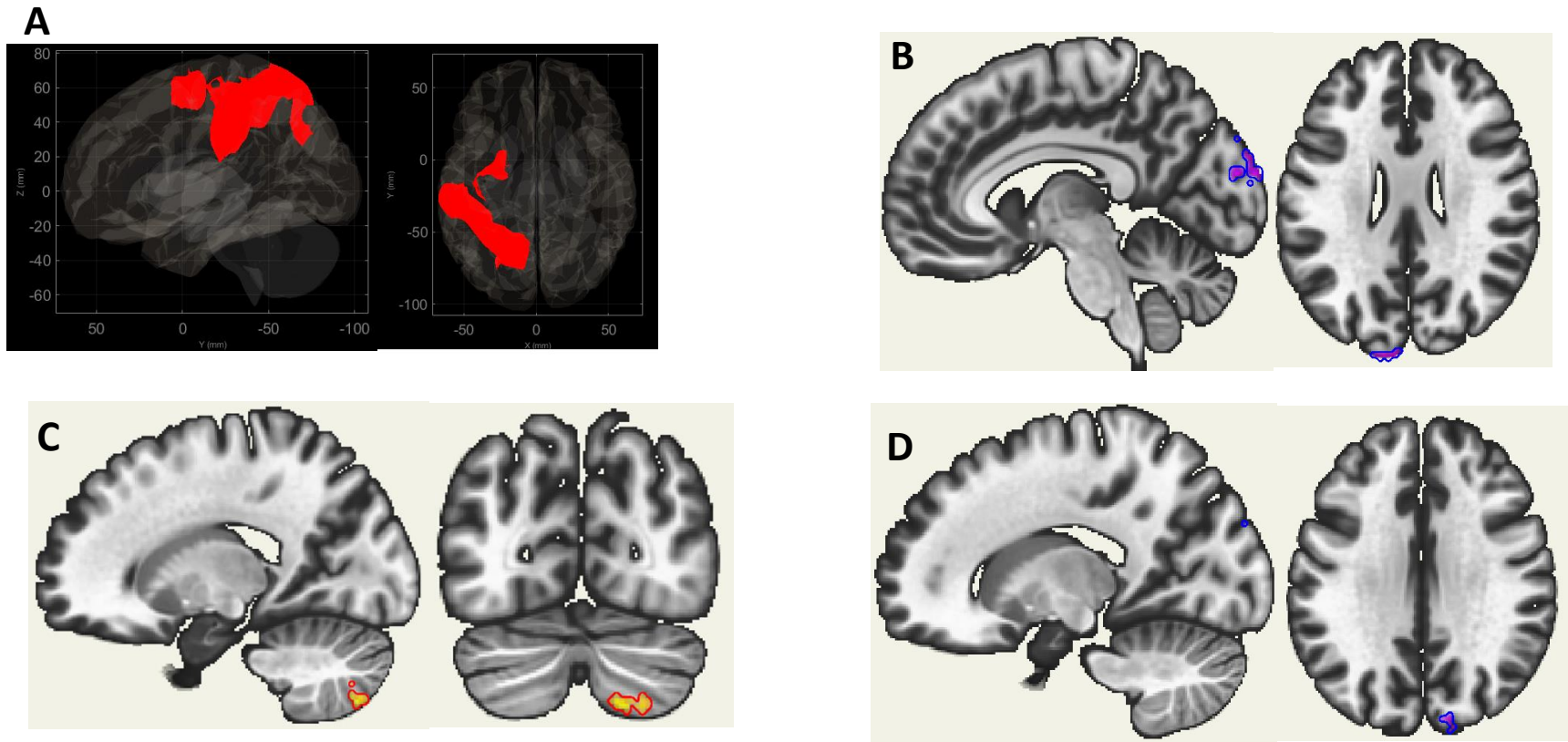
Note. The orientation (axial, sagittal, or coronal) corresponds to the best visualization of clusters. In some cases, visualizations were displayed in a 3D rendered glass brain (distinguished by a black background); two slices would not be a sufficient visualization of the entire cluster. **A)** 90 voxel cluster with peak correlation from (48, 06, 22), located in the right pars opercularis of the inferior frontal gyrus. **B)** 22 voxel cluster with peak correlation from (-48 -12, 54), located in the left precentral gyrus.

Figure 4. Visualization of significant clusters from Dorsal-Attention network – Left frontal eye fields



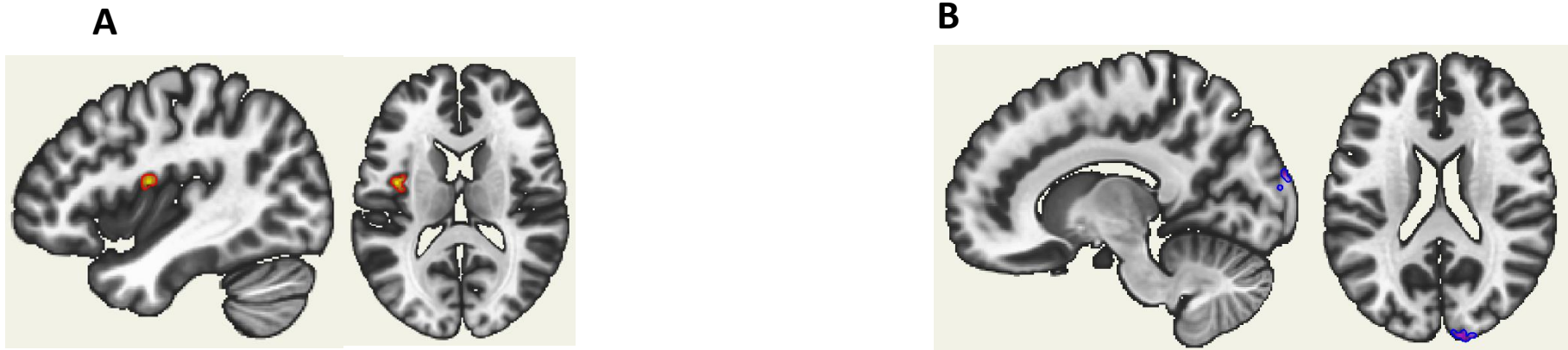
Note. The orientation (axial, sagittal, or coronal) corresponds to the best visualization of clusters. In some cases, visualizations were displayed in a 3D rendered glass brain (distinguished by a black background); two slices would not be a sufficient visualization of the entire cluster. **(A)** 2381 voxel cluster with peak correlation from (-28, -08, 60), located in the left central gyrus and superior parietal lobe. **(B)** 196 voxel cluster with peak correlation from (42, -46, 58), located in the right superior parietal lobe. **(C)** 23 voxel cluster with peak correlation from (-38, -04, 16), located in the left central opercular cortex.

Figure 5. Visualization of significant clusters from Dorsal-Attention network – Left intra-parietal sulcus



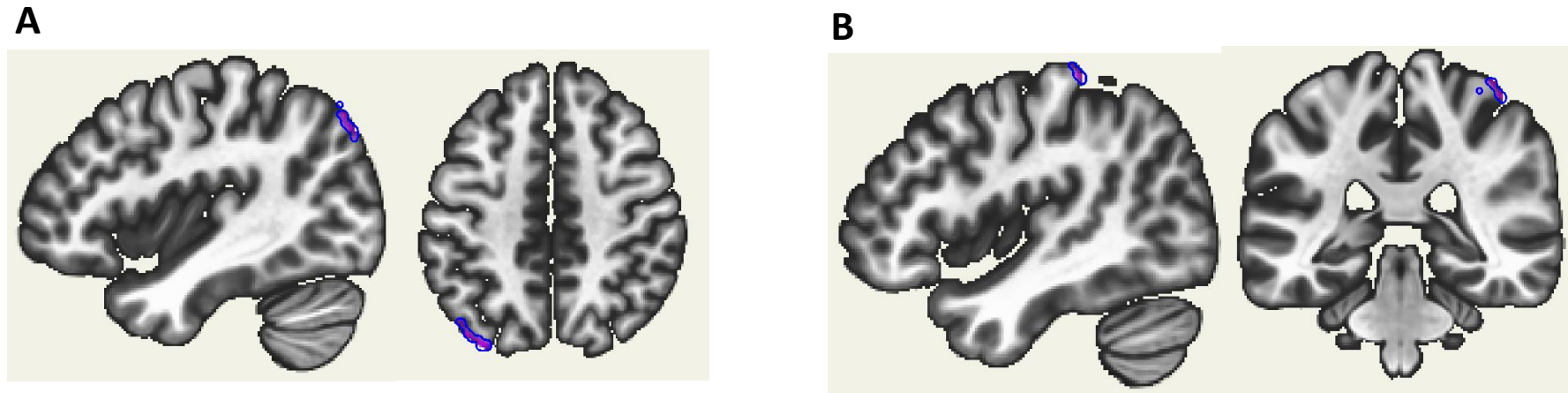
Note. The orientation (axial, sagittal, or coronal) corresponds to the best visualization of clusters. In some cases, visualizations were displayed in a 3D rendered glass brain (distinguished by a black background); two slices would not be a sufficient visualization of the entire cluster. **A)** 4172 voxel cluster with peak correlation from (-62, -24, 42), located in the left postcentral gyrus, superior parietal lobe, supramarginal gyrus, and lateral occipital lobe. **B)** 128 voxel cluster with peak correlation from (-06, -96, 26), located in the left occipital pole. **C)** 59 voxel cluster with peak correlation from (18, -74, -52), located in the right cerebellum8. **D)** 13 voxel cluster with peak correlation from (12, -96, 20), located in the right cerebellum8.

Figure 6. Visualization of significant clusters from Dorsal-Attention network – Right intra-parietal sulcus



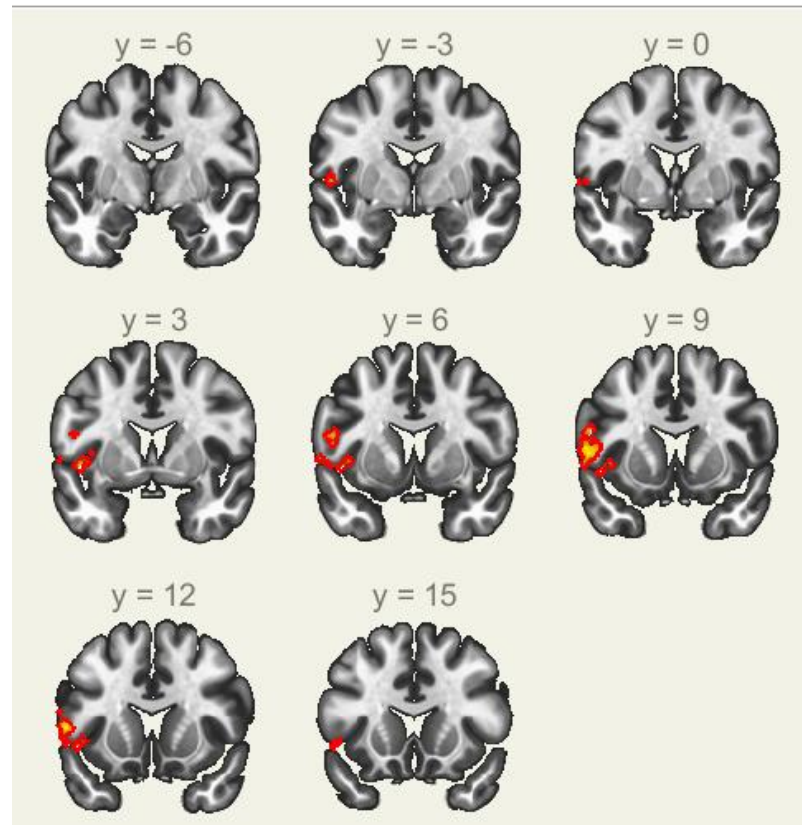
Note. The orientation (axial, sagittal, or coronal) corresponds to the best visualization of clusters. In some cases, visualizations were displayed in a 3D rendered glass brain (distinguished by a black background); two slices would not be a sufficient visualization of the entire cluster. **A)** 32 voxel cluster with peak correlation from (-40, -04, 14), located in the left central opercular cortex. **B)** 20 voxel cluster with peak correlation from (12, -96, 20), located in the right occipital pole.

Figure 7. Visualization of significant clusters from Saliency Network – Left insula



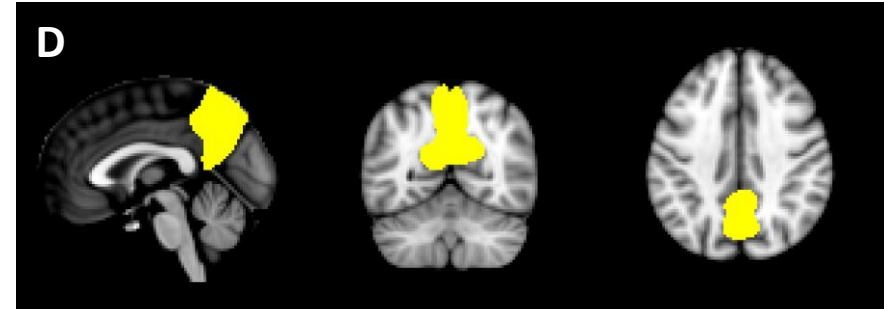
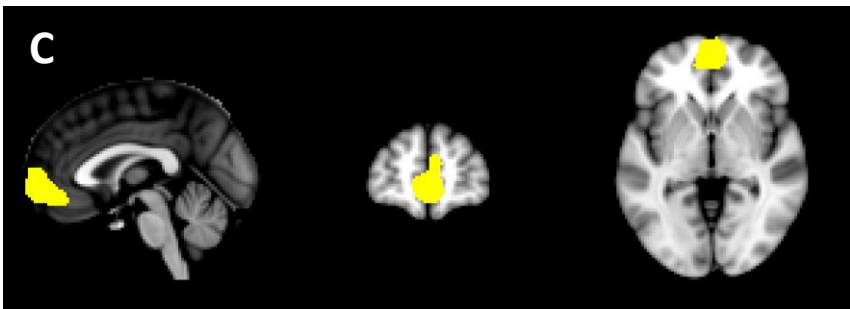
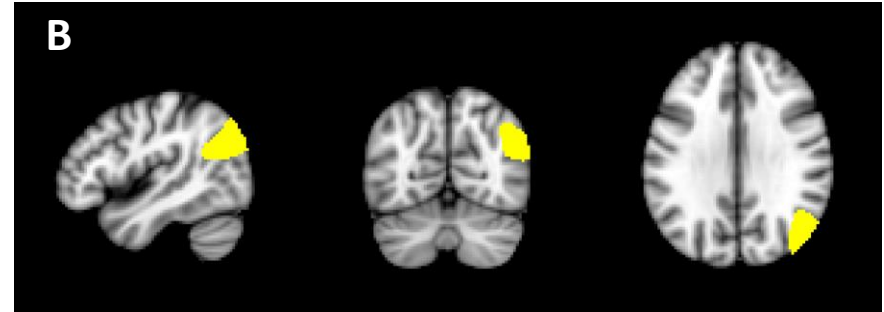
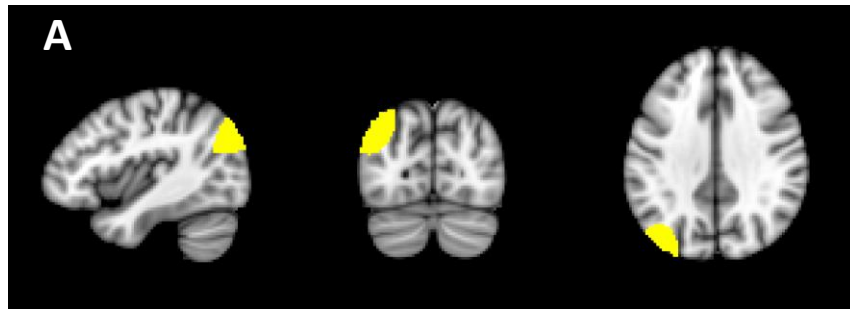
Note. The orientation (axial, sagittal, or coronal) corresponds to the best visualization of clusters. In some cases, visualizations were displayed in a 3D rendered glass brain (distinguished by a black background); two slices would not be a sufficient visualization of the entire cluster. **A)** 66 voxel cluster with peak correlation from (-40, -74, 46), located in the left lateral occipital cortex. **B)** 25 voxel cluster with peak correlation from (44, -34, 62), located in the right postcentral gyrus.

Figure 8. Visualization of significant clusters from Saliency Network – Right supramarginal gyrus



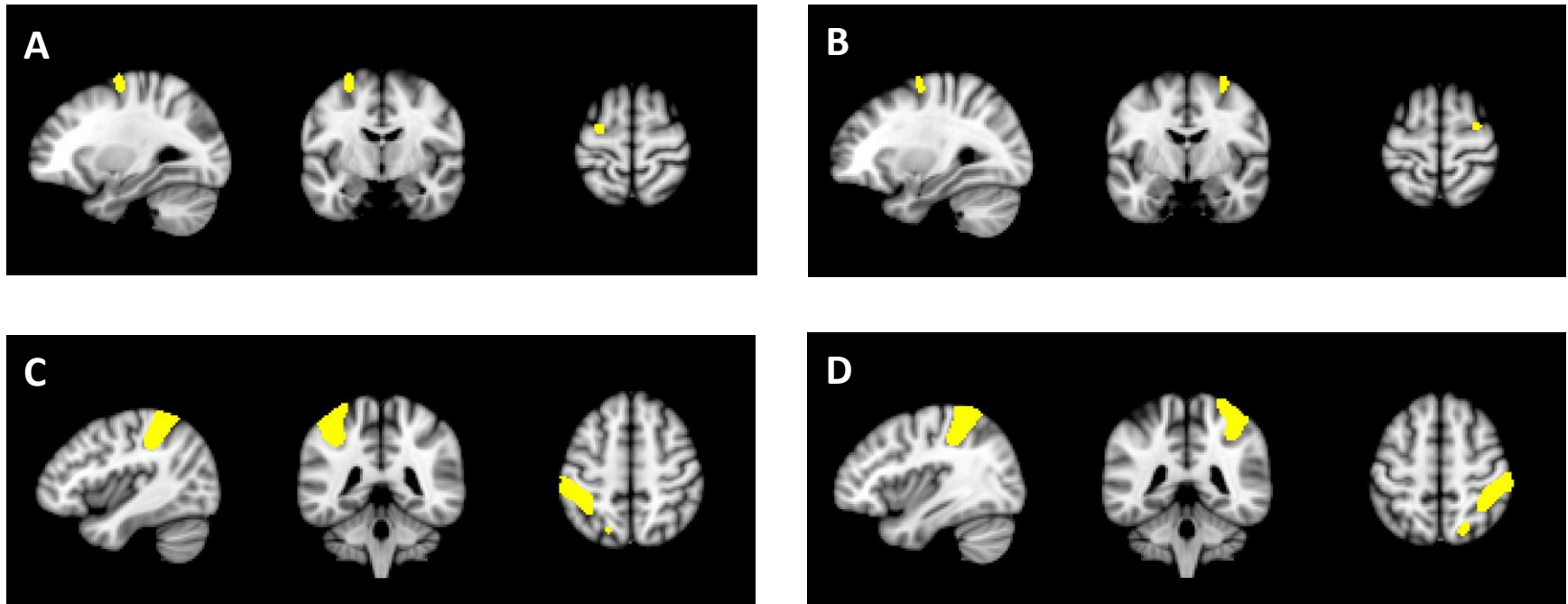
Note. The orientation (axial, sagittal, or coronal) corresponds to the best visualization of clusters. In some cases, visualizations were displayed in a 3D rendered glass brain (distinguished by a black background); two slices would not be a sufficient visualization of the entire cluster. 173 voxel cluster with peak correlation from (-58, 06, 02), located in the pars opercularis of the left inferior frontal gyrus, precentral gyrus, and central opercular cortex.

Figure 9. CONN ROIs – Default Mode Network



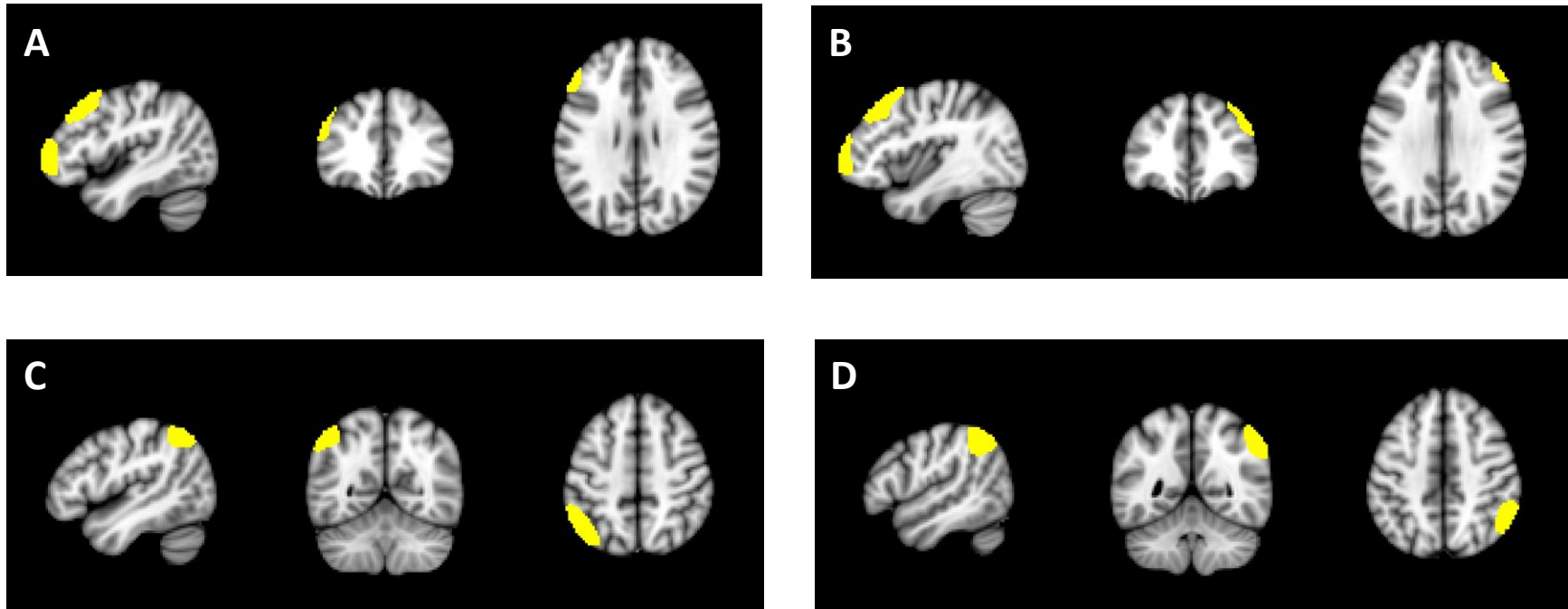
ROI = region of interest. **A)** Left lateral parietal cortex. **B)** Right lateral parietal cortex. **C)** Medial prefrontal cortex. **D)** Posterior cingulate cortex.

Figure 10. CONN ROIs – Task positive network – Dorsal Attention Network



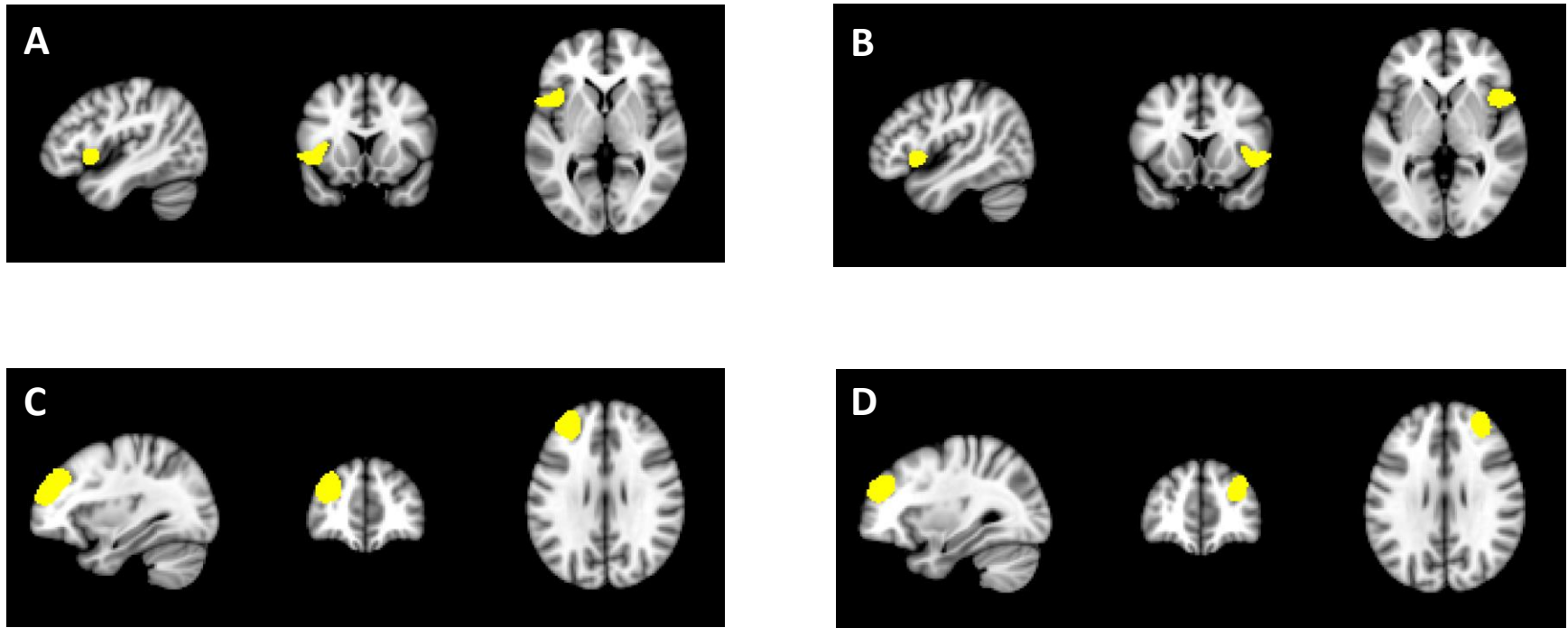
ROI = region of interest. **A)** Left frontal eye fields. **B)** Right frontal eye fields. **C)** Left intra-parietal sulcus. **D)** Right intra-parietal sulcus.

Figure 11. CONN ROIs – Task positive network – Fronto-Parietal Network



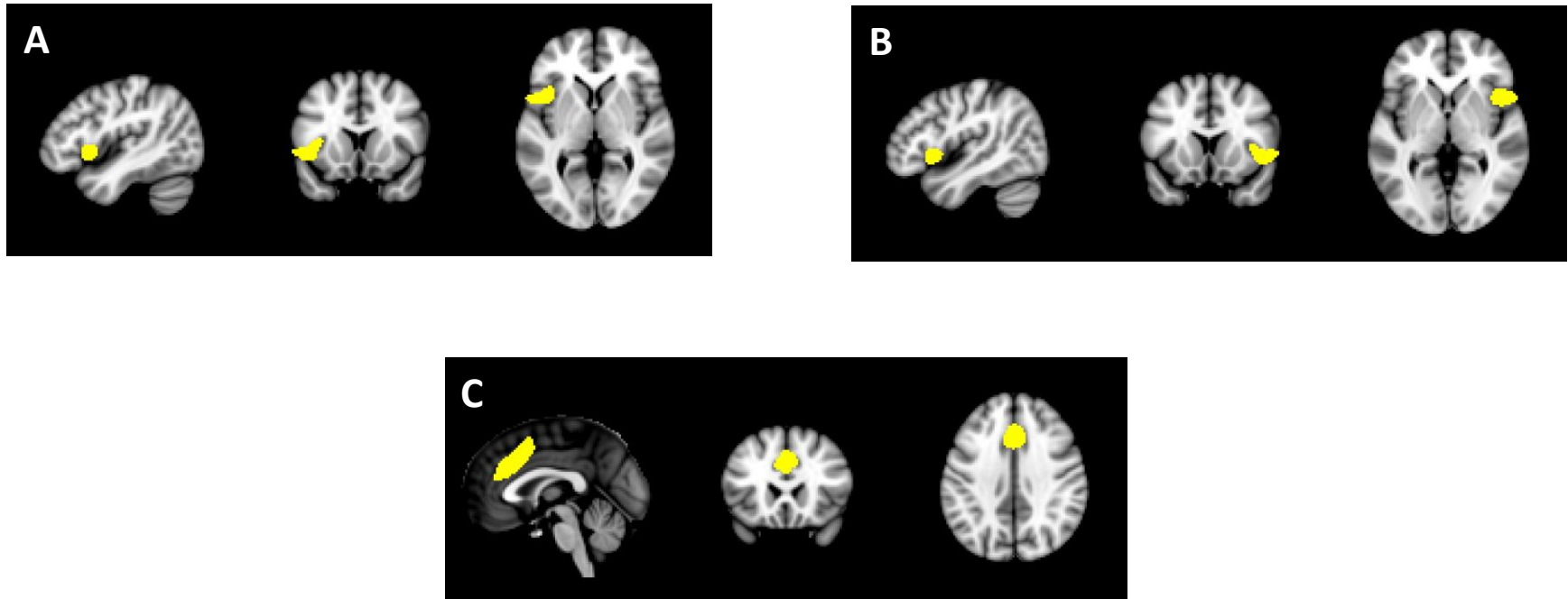
ROI = region of interest. **A)** Left lateral prefrontal cortex. **B)** Right lateral prefrontal cortex. **C)** Left posterior parietal lobe. **D)** Right posterior parietal lobe.

Figure 12a. CONN ROIs – Salience Network



ROI = region of interest. **A)** Left insula. **B)** Right insula. **C)** Left rostral prefrontal cortex. **D)** Right rostral prefrontal cortex.

Figure 12b. CONN ROIs – Salience Network



ROI = region of interest. **A)** Left insula. **B)** Right insula. **C)** Anterior cingulate cortex